

IV. MEDIUM-ENERGY NUCLEAR PHYSICS RESEARCH

OVERVIEW

The overall goals of the Medium-Energy Physics research program in the Argonne Physics Division are to test our understanding of the structure of hadrons and the structure of nuclei, and to develop and exploit new technologies for high-impact applications in nuclear physics as well as other national priorities. In order to test our understanding of the structure of hadrons and the structure of nuclei within the framework of quantum chromodynamics, the medium-energy research program emphasizes the study of nucleons and nuclei on a relatively short distance scale. Because the electromagnetic interaction provides an accurate, well-understood probe of these phenomena, primary emphasis is placed on experiments involving electron scattering, real photons and Drell-Yan processes. The electron beams of the Thomas Jefferson National Accelerator Facility (TJNAF) are ideally suited for studies of nuclei at hadronic scales and represent one center of the experimental program. Staff members led in the construction of experimental facilities, serve as spokespersons or co-spokespersons for 16 experiments and are actively involved in several others. The group constructed the broad-purpose Short Orbit Spectrometer which forms half of the coincidence spectrometer pair that is the base experimental equipment in Hall C. We continue to improve the understanding of the spectrometer optics and acceptance. We will have a major role in re-establishing the SOS in Hall C this Spring for a series of five upcoming experiments. Argonne led the first experiment to be carried out at TJNAF in FY1996 and has completed eleven other experiments.

Recently, staff members have focused increasingly on studies of the nucleon. In FY2002 measurements were made on the ratio of the electromagnetic elastic form factors of the proton using a modified Rosenbluth method. These results will provide an important check of the polarization-transfer results that disagree so markedly from data recorded previously with the traditional Rosenbluth method. In FY2000, the exclusive cross sections from charged photopion production on the neutron and proton were measured up to a photon energy of 5.6 GeV as a test

of “transition region” models which describe the transition from hadronic degrees of freedom to quark-gluon degrees of freedom. Surprisingly, the results are consistent with predictions of pQCD even at these relatively low energies. Early in FY2003 measurements of polarization were performed for two-body photodisintegration of the deuteron at high energy. Measurements of kaon production on light nuclei provide important information on the basic strangeness production mechanisms and the poorly known low energy hyperon-nucleon interaction. A new initiative to search for color transparency in rho production in nuclei was approved by the JLab Program Advisory Committee and is scheduled to begin in July, 2003 in Hall B at JLab. This work represents an important extension of Argonne’s earlier rho electro-production studies at HERMES.

HERMES, a broadly based North American-European collaboration is studying the spin structure of the nucleon using internal polarized targets in the HERA storage ring at DESY. Deep inelastic scattering has been measured with polarized electrons on polarized hydrogen, deuterium and ^3He . Argonne has concentrated on the hadron particle identification of HERMES, a unique capability compared to other spin structure experiments. In 1999 and under Argonne leadership, the dual-radiator ring imaging Cerenkov counter (RICH) was brought into operation at the design specifications to provide complete hadron identification in the experiment. The RICH has been operating routinely since its installation. This has allowed HERMES to make decisive measurements of the flavor dependence of the spin distributions. Subsequently, HERMES has performed a five-component decomposition of the proton’s spin structure function and the first measurement of the x-dependence of the strange sea polarization. In addition, HERMES provided the first direct indication of a positive gluon spin contribution to the nucleon. Recent HERMES rho electro-production data were consistent with the concept of color transparency. A follow-up experiment will be performed in Hall B at JLab to confirm or deny this finding. Recently, HERMES has provided the first measurement of the b_1 structure function of the deuteron. During 2001, HERMES installed a transversely polarized target and is poised to provide the first measurements of the transversity structure function of the proton.

Measurements of high mass virtual photon production in high-energy proton-induced reactions have determined the flavor dependence of the sea of antiquarks in the nucleon. These measurements give insight into the origin of the nucleon sea. In the same experiment, the high-x absolute Drell-Yan cross sections were measured. These results demonstrate that modern high-x parton distributions are significantly in error. In FY01, a new initiative was approved by the FNAL PAC to continue these measurements with much higher luminosity at the FNAL Main Injector. These Drell-Yan experiments not only provide the best means to measure anti-quark distributions in the nucleon and nuclei, but represent an outstanding opportunity to perform these measurements at an ideal proton beam energy of 120 GeV.

The technology of laser atom traps provides a unique environment for the study of nuclear and atomic systems and represents a powerful new method that is opening up exciting new opportunities in a variety of fields, including nuclear physics. The group has developed a high-efficiency, high-sensitivity magneto-optical trap for rare, unstable isotopes of krypton. The group has collected and purified ancient ground water from the Nubian aquifer in Egypt. Cross checks with low-level counting techniques for ^{85}Kr have validated the new technique. For the first time, the group has trapped a single atom of ^{41}Ca from purified urine samples from patients who have ingested a ^{41}Ca tracer. This is a necessary first step to develop a new method for measuring rates of bone loss in humans. Recently, an optical trap was constructed and tested for the purpose of measuring the charge radius of ^6He at ATLAS. This trap will be moved and re-established in the BGO area at ATLAS in preparation for the experiment.

A new initiative to search for an electric dipole moment (EDM) of ^{225}Ra was begun during the past year. The ultimate goal is to search for a non-zero EDM for ^{225}Ra and improve the sensitivity for nuclear EDM searches by approximately two orders of magnitude. This test of time-reversal symmetry represents an outstanding opportunity to search for new physics beyond the Standard Model. A new optical trapping laboratory for radium is being established for this experiment. In addition, an exploratory study is underway to determine the feasibility of measuring $\sin^2\theta_w$ in parity violating deep inelastic electron scattering from deuterium at either Jefferson Lab or SLAC.



A. NUCLEON PROPERTIES

a.1. New Measurement of (G_E/G_M) for the Proton (J. Arrington, D. F. Geesaman, K. Hafidi, R. J. Holt, H. E. Jackson, D. H. Potterveld, P. E. Reimer, E. C. Schulte, K. Wijesooriya, B. Zeidman, and the E01-001 collaboration)

The structure of the proton is a matter of universal interest in nuclear and particle physics. Charge and current distributions are obtained through measurements of the electric and magnetic form factors, $G_E(Q^2)$ and $G_M(Q^2)$. These form factors can be separated by measuring elastic electron-proton scattering at two or more values of the virtual photon polarization parameter ε (*i.e.* by performing a Rosenbluth separation). Several such measurements have been made, and global fits to these measurements¹ showed that the ratio of G_E to G_M was consistent with unity, indicating equal distributions of charge and magnetization within the proton. Recent measurements at Jefferson Laboratory² used a recoil polarization measurement to extract G_E/G_M at large values of Q^2 . They found that the ratio of $\mu_p G_E/G_M$ was unity at low Q^2 , but fell linearly with increasing Q^2 , reaching a value of 0.3 at $Q^2=5.5 \text{ GeV}^2$ (see Fig IV-1).

It was initially suggested that the Rosenbluth data were unreliable at large Q^2 based on the inconsistency of form factors extracted from various Rosenbluth separations. A re-examination of the cross section measurements shows that the inconsistency is a result of the incomplete treatment (or lack of treatment) of normalization uncertainties when data from different experiments are combined to extract the form factors. When the normalization uncertainties are properly included, or when the form factors are extracted from a single data set, the results are not inconsistent. In addition, we performed a global reanalysis of the world's e-p cross section data, and find that the discrepancy is not the result of errors in a single data set, nor can it be explained by 'reasonable' adjustments of the experimental normalization factors.³ In order to be confident in our knowledge of the proton form factors, we must determine not only which result is correct, but also why these two techniques disagree. A systematic problem with either set of measurements

would most likely affect other measurements which use the same techniques.

Experiment E01-001⁴ was performed at Jefferson Lab in May 2002. Data were taken to allow a Rosenbluth extraction of G_E/G_M in the range where the previous data disagree with the recoil polarization measurements. The goal is to have a single data set that will provide a high-precision measurement of the ratio, with careful tests of the systematic uncertainties. In addition to careful monitoring of potential uncertainties, this measurement used a different experimental technique which significantly decreased our sensitivity to the systematics that have limited previous measurements.

The main difference in this measurement is that we detected the struck proton, rather than the scattered electron. Detecting the proton means that there is no ε -dependence to the momentum of the detected particle, much less rate-dependence, and significantly less sensitivity to uncertainties in the beam energy or scattering angles. Finally, the radiative corrections are smaller, and have less ε dependence.

The other unusual feature of this measurement is that while we perform a Rosenbluth extraction at high- Q^2 in one spectrometer, we will make a simultaneous measurement at low Q^2 . Because the value of G_E/G_M at low Q^2 is relatively well known, and because the kinematics chosen make the low Q^2 measurement insensitive to the photon polarization ($\Delta\varepsilon$ is kept small), we can use the low Q^2 point as a pseudo-luminosity monitor to correct for any error in the beam charge and target thickness measurements.

¹R. C. Walker *et al.*, Phys. Rev. D **49**, 5671 (1994).

²M. K. Jones *et al.*, Phys. Rev. Lett. **84**, 1398 (2000); O. Gayou *et al.*, Phys. Rev. C **64**, 038292 (2001); O. Gayou *et al.*, Phys. Rev. Lett. **88**, 092301 (2002).

³J. Arrington, preprint, hep-ph/0209243.

⁴Jefferson Lab Experiment E01-001, 'New Measurement of (G_E/G_M) for the Proton', J. Arrington and R. E. Segel, spokespersons.

Figure IV-1 shows the existing Rosenbluth and recoil polarization results, along with projected uncertainties for E01-001 for two cases: $\mu_p G_E/G_M = 1$, and $\mu_p G_E/G_M$ consistent with the polarization measurements. If the results agree with previous Rosenbluth extractions, then it will still be unclear which technique is correct, but we will rule out several of the most likely causes for systematic errors in the previous Rosenbluth

extractions. If we agree with the polarization transfer measurements, we will be sure of the $\mu_p G_E/G_M$ results extracted by this technique, and will have identified the likely causes for the discrepancy with the standard Rosenbluth measurements. The analysis of the data is currently underway at Argonne, and we expect preliminary results in 2003.

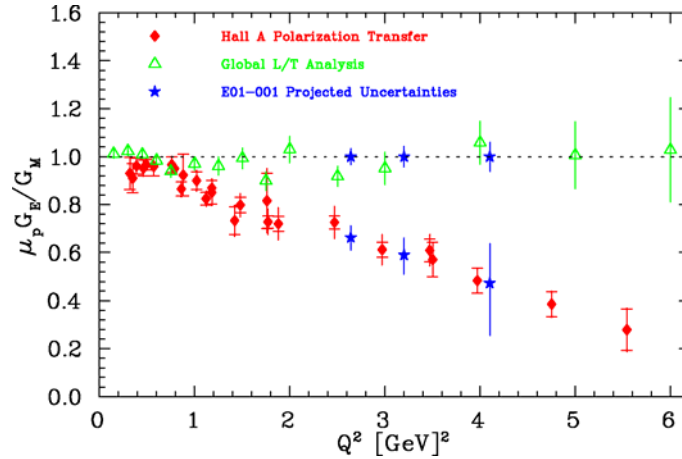


Fig. IV-1. Existing measurements of $\mu_p G_E/G_M$ along with projected uncertainties for this experiment. Uncertainties are shown for results consistent with form factor scaling, and for results consistent with the polarization transfer results.

a.2. Separated and Unseparated Structure Functions in the Nucleon Resonance Region (J. Arrington, D. F. Geesaman, R. J. Holt, T. G. O'Neill, D. H. Potterveld, and the E99-119, E00-002, and E00-116 collaborations)

A great deal of our understanding of the quark substructure of the nucleon comes from inclusive electron scattering. Reliable *global* descriptions of inclusive electroproduction data are necessary for electron-nucleon scattering model development, accurate radiative correction calculations, and the extraction of form factors, structure functions, and parton distribution functions from inclusive electron scattering experiments. However, most measurements have focused on the deep inelastic region. High precision cross section measurements in the resonance region, combined with a separation of the longitudinal σ_L and transverse σ_T components, will substantially improve the global description of electroproduction at moderate to high Q^2 and large Bjorken- x . While the ratio $R = \sigma_L/\sigma_T$ has been measured up to high Q^2 for elastic and deep inelastic scattering, there exist few measurements of R in the resonance region at moderate or high

momentum transfers. The current uncertainty in R in the resonance region is greater than 100%. Experiment E94-110¹ ran in 1999 in Hall C at Jefferson Lab, and made a precision measurement of R in the resonance region, up to $Q^2 = 4.5 \text{ GeV}^2$.

Previous JLab measurements of inclusive scattering in the resonance region, measuring just the F_2 structure function, have been analyzed in terms of Local Duality. It was observed that the resonance region data, when averaged over the Nachtmann variable, ξ , reproduced the structure function as measured in the deep inelastic region². This duality of the DIS and resonance structure function held to better than 10%, down to $Q^2 = 0.5 \text{ GeV}^2$. It was also observed that at low ξ , the resonance region structure function deviated from the DIS value, and showed a valence-like behavior³, going to zero as ξ decreased. While this duality has been

observed for hydrogen, deuterium, and nuclear targets for F_2 , no such data existed for the F_1 structure function in the resonance region. The new results from E94-110 yield a high-precision measurement of R in the resonance region, and also show that duality holds in both the F_2 and F_1 structure functions (see Fig. IV-2). In addition, the data show for the first time longitudinal contributions to the resonance electroproduction. These data will allow improved extractions of the transition form factors from inclusive measurements, which usually involves assuming that the resonance production occurs only in the transverse channel.

Future experiments, three of which are scheduled to run in 2003, will further extend these duality measurements. There is an approved experiment to extend duality studies of F_2 on hydrogen and deuterium to $Q^2 = 7.5 \text{ GeV}^2$, another to make measurements at low x and Q^2 to study the valence-like nature of the resonance region structure function, and a measurement of duality in semi-inclusive pion production ('tagged' electron scattering). In addition, there is an approved experiment to perform a similar Rosenbluth separation in the resonance region for deuterium.

¹JLab experiment E94-110, 'Measurement of $R=\sigma_L/\sigma_T$ in the Nucleon Resonance Region', C. E. Keppel, spokesperson.

²I. Niculescu *et al.*, Phys. Rev. Lett. **85**, 1182 (2000).

³I. Niculescu *et al.*, Phys. Rev. Lett. **85**, 1186 (2000).

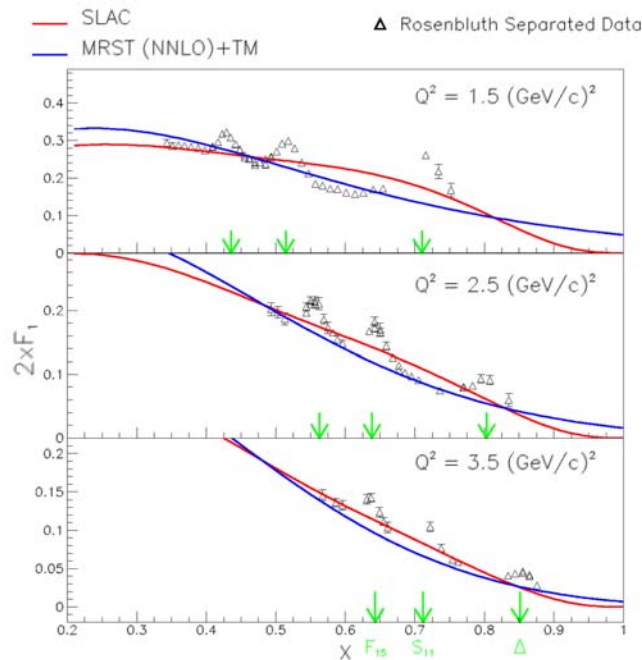


Fig. IV-2. The separated structure function, $2xF_1$, as a function of x for three Q^2 bins, compared to a SLAC parameterization for DIS and a NNLO calculation using MRST parton distribution functions and target mass corrections.

a.3. Charged Pion Photoproduction From the Nucleon (R. J. Holt, J. Arrington, K. Bailey, P. E. Reimer, F. Dohrmann, K. Hafidi, T. O'Connor, E. C. Schulte, K. Wijesooriya, and JLab E94-104 Collaboration)

The goal of experiment E94-104 is to measure the cross sections for the $\gamma n \rightarrow \pi^- p$ and the $\gamma p \rightarrow \pi^+ n$ reactions for photon energies up to 5.5 GeV and at several reaction angles. The experiment was completed and the data are nearing the final analyses. From these data, the π^-/π^+ ratio can be formed and compared with existing models. One of the most celebrated models of the

transition region from hadronic degrees of freedom to the quark-gluon degrees of freedom is represented by a one-hard gluon exchange diagram. This model gives a definite prediction¹ for the ratio:

$$\frac{d\sigma(\gamma n \rightarrow \pi^- p)}{d\sigma(\gamma p \rightarrow \pi^+ n)} = \left(\frac{ue_d + se_u}{ue_u + se_d} \right)^2$$

where the e_i are the charges of the quarks, and s and u are the usual Mandelstam variables. The data at $\theta_{\text{cm}} = 90^\circ$ are shown in Fig IV-3. The cross sections for both the reactions are consistent with the constituent counting rules at the highest energies, while the ratio at

the highest energies is consistent with the pQCD prediction. The results are in remarkable agreement with pQCD; however, data should be taken at higher energies to confirm this trend. The results also indicate a rather broad, resonance-like structure near $s = 5 \text{ GeV}^2$, which should be further investigated with complete angular distribution and polarization measurements. The data at other angles are presently undergoing analysis.

¹H. Huang and P. Kroll, Eur. Phys. J. C17, 423 (2000).

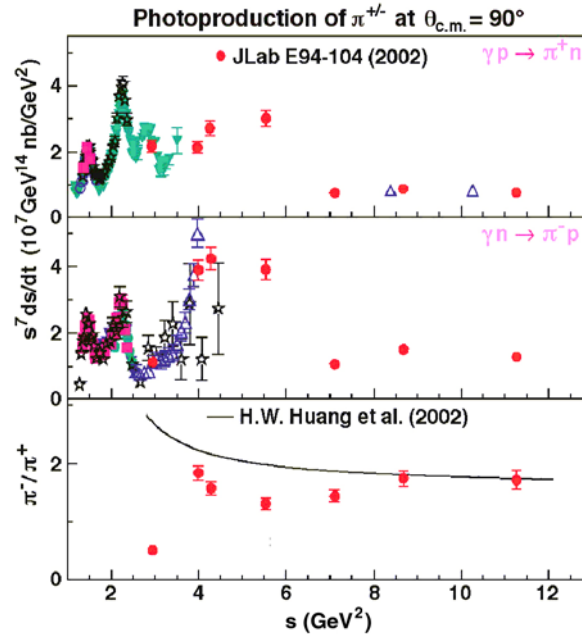


Fig. IV-3. The two upper panels display the quantities $s^7 d\sigma/dt$ as a function of s for the $\gamma p \rightarrow \pi^+ n$ and the $\gamma n \rightarrow \pi^- p$ reactions, respectively. The ratio of these two cross sections is shown in the lower panel along with the pQCD prediction of Huang and Kroll.

a.4. Search for QCD Oscillations in the $\gamma N \rightarrow \pi N$ Reactions (R. J. Holt, J. Arrington, D. F. Geesaman, H. E. Jackson, P. E. Reimer, K. Hafidi, E. C. Schulte, K. Wijesooriya, and JLab E02-010 Collaboration)

A proposal to search for QCD oscillations in exclusive charged photopion reactions was approved by the Jefferson Laboratory Program Advisory Committee. The goal of the experiment is to search in photopion reactions for the oscillatory effect observed in exclusive high-energy proton-proton elastic scattering. In p-p elastic scattering the cross section was found to oscillate about the $1/s^{10}$ dependence expected from the constituent counting rules. This oscillatory behavior has been ascribed¹ to a short distance (hard-scattering) amplitude which interferes with a long-distance

amplitude (Landshoff). This process is analogous to coulomb-nuclear interference observed in low energy charged particle scattering; however, the QCD oscillations arise from soft gluon radiation rather than from photon radiation as in the QED case. This interference also can give rise to polarizations observed in high energy exclusive hadron-hadron scattering processes. In the proposed experiment, the cross sections will be measured in a fine energy scan up to the highest energy available at Jefferson Lab.

¹S. J. Brodsky, C. E. Carlson, and H. Lipkin, Phys. Rev. D 20, 2278 (1979); J. P. Ralston and B. Pire, Phys. Rev. Lett. 65, 2343 (1990).

B. SUBNUCLEONIC EFFECTS IN NUCLEI

b.1. Proton Polarization Angular Distribution in Deuteron Photodisintegration

(R. J. Holt, J. Arrington, K. Hafidi, P. E. Reimer, E. C. Schulte, K. Wijesooriya, and JLab E00-007 Collaboration)

The overall goal of experiment E00-007 is to determine the mechanism that governs photoreactions in the GeV energy region. Our previous measurements¹ of induced polarization in deuteron photodisintegration produced surprising results at photon energies between 1 and 2 GeV. First these results disagreed markedly with previous experiments and secondly there was a remarkable disagreement with the meson-exchange model. The induced polarizations above 1 GeV and at $\theta_{\text{cm}} = 90^\circ$ were near zero, consistent with hadron

helicity conservation.; however, it might be expected that the results could have been accidentally zero because of a $\sin(n\theta)$ dependence where n happens to be even. Thus, the goal of this experiment was to determine the angular dependence of the polarization. The experiment was completed in October 2002 and data were taken at five center-of-mass angles: 37° , 53° , 70° , 90° and 110° . The induced polarizations as well as polarization transfers were measured. Presently, the data are undergoing analysis.

¹K. Wijesooriya *et al.*, Phys. Rev. Lett. **86**, 2975 (2001).

b.2. Measurement of the Transparency Ratio for the $A(\gamma, \pi^- p)$ Reaction in Helium and Deuterium

(R. J. Holt, J. Arrington, K. Bailey, P. E. Reimer, F. Dohrmann, K. Hafidi, T. O'Connor, E. C. Schulte, K. Wijesooriya, and JLab E94-104 Collaboration)

The transparency for the ${}^4\text{He}(\gamma, \pi^- p)$ reaction compared with the $D(\gamma, \pi^- p)p$ reaction was measured as a function of photon energy in Hall A at Jefferson Laboratory. The fundamental process $\gamma n \rightarrow \pi^- p$ exhibits a scaling behavior consistent with the constituent counting rules above a photon energy of 2.5 GeV. Thus, one can use

this reaction in the nuclear medium to determine whether the onset of color transparency has been observed. The pion is expected¹ to exhibit the phenomenon of color transparency more readily than the proton since the pion has only two constituent partons. The data are presently being analyzed.

¹B. Blättel *et al.*, Phys. Rev. Lett. **70**, 896 (1993).

b.3. Measurements of the Nuclear Dependence of $R = \sigma_L/\sigma_T$ at Low Q^2

(J. Arrington, D. F. Geesaman, T. G. O'Neill, D. H. Potterveld, and the E99-118 Collaboration)

Inclusive electron scattering is a well understood probe of the partonic structure of nucleons and nuclei. Deep inelastic scattering has been used to make precise measurements of nuclear structure functions over a wide range in x and Q^2 . The ratio $R = \sigma_L/\sigma_T$ has been measured reasonably well in deep inelastic scattering at moderate and high Q^2 using hydrogen and deuterium targets. However, R is still one of the most poorly understood quantities measured in deep inelastic scattering and few measurements exist at low Q^2 or for nuclear targets. Existing data rule out significant nuclear effects in R only at moderate to large values of Q^2 .

Jefferson Lab Experiment E99-119 is a direct measurement of R at low x and low Q^2 . The experiment was performed in July of 2000 and data was taken for hydrogen, deuterium, and heavier nuclei. The data are largely analyzed, but the cross section extraction at extremely small values of x and Q^2 involve large radiative corrections. While the radiative corrections will limit the region for which R can be extracted, these data are ideal for testing the radiative correction procedures in these extreme kinematics, and in particular the corrections coming from the nuclear elastic contributions.

b.4. Electroproduction of Kaons and Light Hypernuclei (J. Arrington, K. Bailey, F. Dohrmann, D. F. Geesaman, K. Hafidi, B. Mueller, T. G. O'Neill, D. H. Potterveld, P. Reimer, B. Zeidman, and the E91-016 Collaboration)

Jefferson Lab experiment E91-016, "Electroproduction of Kaons and Light Hypernuclei" is a study of the production of Kaons on targets of H, D, ^3He , and ^4He at an incident electron energy of 3.245 GeV and $Q^2 \approx 0.37 \text{ GeV}^2$. For H and D targets, additional data were obtained at an energy of 2.445 GeV and $Q^2 \approx 0.5 \text{ GeV}^2$. The scattered electrons and emergent kaon were detected in coincidence with the use of the HMS and SOS spectrometers in Hall C. Particle identification utilizing time-of-flight techniques together with Aerogel Cerenkov detectors provided clean missing-mass spectra and allowed subtraction of random backgrounds. In addition to obtaining spectra, angular distributions were measured at forward angles with respect to the virtual photons.

The fundamental interaction being studied is the $N(e,e'K^+)Y$ where Y is either Λ or Σ and N is a nucleon, either free or bound in a nucleus. For H, the final state can only be a Λ or Σ^0 , with a missing mass spectrum consisting of two sharp peaks. For heavier targets, however, not only can Σ^- be produced on the neutron, but the relative motion of the bound nucleons results in quasi-free broadening of the peaks. Since there is no known bound state in the mass 2 hyper-nuclear system, only quasi-free production is observed. For the heavier targets, $^3,^4\text{He}$, both Fermi broadening and a rapidly increasing number of final state configurations makes it more difficult to separate the various contributions. Because of the small mass difference between Σ^0 and Σ^- , distinguishing between these contributions is not possible without assuming that the Λ/Σ^0 ratio is the same as that for the free proton. Subtraction of the normalized Σ^0 contribution yields a value for Σ^- production on the neutron. The ratio of cross sections, Σ^0/Σ^- , suggests s-channel dominance for the $D(e,e'K^+)$ reaction in the present kinematic regime.

The analyses of the data for ^4He provide unambiguous evidence for the formation of the bound hypernucleus hyper- ^4H ; the first observation of electroproduction of a hyper-nuclear bound state. From other reactions, a 1^+ excited state bound by $\sim 1 \text{ MeV}$ is known to exist in

this nucleus; the 0^+ ground state is bound by 2.04 MeV. For ^3He , the evidence for the electroproduction of the hypertriton, *i.e.* the p-n Λ state bound by $\sim 130 \text{ keV}$, is less convincing. While barely discernible near zero degrees, because of kinematic effects, the bound state becomes more evident away from zero degrees.

Extraction of cross sections for specific channels becomes more difficult with increasing mass because of the rapidly growing number of possible final configurations. However, the various models that have been utilized for the helium isotopes yield simulations that are in reasonable agreement with the shapes of the spectra. Since it is not possible to distinguish between Σ^0 and Σ^- production, the analyses assume the Λ/Σ^0 ratio data for H obtained at the same laboratory settings as input to extract the Σ^- yields. Further analyses of these results are in progress.

In addition, the excellent particle identification allowed an ancillary study of the electroproduction of ω mesons on the proton. The relatively large cross section for this process, combined with kinematic focusing of the residual protons, provided high yields and excellent statistical accuracy over a wide range of c.m. angles. A representative missing mass spectrum is shown in Fig. IV-4. The data result in new insights into the fundamental production mechanisms.

E91-016 was a high-statistics study of Kaon electroproduction on the light nuclei ^2H , ^3He , and ^4He . During the course of the experiment, extensive data were obtained for the H target as well as additional calibration data for C and Al. These latter data have been analyzed to ascertain the general mass dependence of the cross section for Kaon electroproduction. E91-016 has provided all or a substantial fraction of the thesis data for five students from Hampton University, University of Pennsylvania, and Temple University.

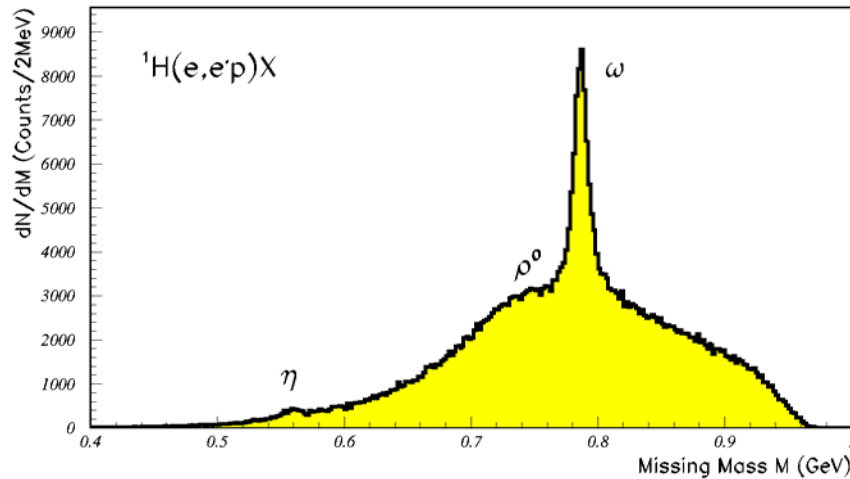


Fig. IV-4. Missing mass spectrum for light vector meson electroproduction, showing signals from η , ρ^0 , and ω production.

b.5. Measurement of the EMC Effect in Very Light Nuclei (J. Arrington, F. Dohrmann, D. Gaskell, D. F. Geesaman, K. Hafidi, R. J. Holt, H. E. Jackson, D. H. Potterveld, P. E. Reimer, B. Zeidman, and the E00-101 collaboration)

In nuclei, the quark momentum distribution varies with the density of the nucleus. The structure function is suppressed in heavy nuclei at large values of x (corresponding to large quark momenta), and enhanced at low x values. Measurements to date indicate that the overall form of this modification is the same for all nuclei, but the magnitude of the enhancement and suppression is larger for heavier nuclei. Many attempts have been made to explain the EMC effect, but none of the proposed models can fully reproduce the observed modifications, and there is still no consensus on which effect or combination (if any) explain the data.

Experiment E00-101¹ will measure the EMC effect for ${}^3\text{He}$ and ${}^4\text{He}$. The current data cannot distinguish different models of the density dependence of the effect. Because ${}^4\text{He}$ has an anomalously large density for a light nucleus, it is the most sensitive test to determine if the EMC effect scales with A or with nuclear density. More importantly, these measurements of the EMC effect can be compared to exact few body calculations. If the EMC effect is caused by few

nucleon interactions, the universal shape observed in heavy nuclei may be a result of a saturation of the effect, and the shape may be different in few-body nuclei. While the existing data on heavy nuclei all show the same x -dependence, there are calculations that predict significantly different dependences for very light nuclei. By making precise measurements in light nuclei, we will be able to distinguish between different models of the EMC effect based on their predictions for few-body nuclei.

Finally, a measurement of $A \leq 4$ nuclei will help constrain models of the EMC effect in deuterium. Models of nuclear effects in deuterium and ${}^3\text{He}$ must be used to extract information on neutron structure, and a high precision measurement including ${}^1\text{H}$, ${}^2\text{H}$, ${}^3\text{He}$, and ${}^4\text{He}$ will give a single set of data that can be used to evaluate these models in several light nuclei. This will help to quantify the model dependence of the neutron structure functions inferred from measurements on ${}^2\text{H}$ and ${}^3\text{He}$.

¹Jefferson Lab Experiment E00-101, 'A Precise Measurement of the Nuclear Dependence of Structure Functions in Light Nuclei', J. Arrington, spokesperson.

b.6. Measurement of High Momentum Nucleons in Nuclei and Short Range Correlations
(J. Arrington, D. F. Geesaman, K. Hafidi, R. J. Holt, H. E. Jackson, P. E. Reimer,
E. C. Schulte, and the E02-019 collaboration)

Inclusive scattering from nuclei at low energy transfer (corresponding to $x > 1$) is dominated by quasielastic scattering from nucleons within the nucleus. As the energy transfer is decreased, the scattering probes nucleons of increasing momentum and we can map out the distribution of high momentum nucleons in nuclei. Experiment E89-008¹ measured inclusive scattering for deuterium, carbon, iron, and gold at $x > 1$ using 4 GeV electrons at Jefferson Lab. These data can be used to constrain the high momentum components of nuclear spectral functions. In addition, as the high momentum nucleons are dominantly generated by short range correlations (SRCs), these data allows us to examine the strength of two-nucleon correlations in heavy nuclei.

Experiment E02-019² will extend these measurements to higher values of x and Q^2 using the 6 GeV electron beam at JLab. In addition to measuring scattering from deuterium and heavy nuclei, data will be taken on ³He and ⁴He. The higher Q^2 values in this experiment should simplify the extraction of the high momentum components, as effects such as final state interactions should be reduced as Q^2 is increased. Measurements with few-body nuclei (²H, ³He, and ⁴He) allow contact with theoretical calculations via essentially "exact" calculations for few-body systems. This can be used to study in detail contributions to the interaction beyond the impulse approximation (*e.g.* final state interactions). Data on heavy nuclei can then be used to constrain the high momentum components of their spectral functions, as well as allowing an extrapolation to nuclear matter.

The extension to higher energies will provide us will significantly greater sensitivity to the high momentum components of the nuclear wave function, probing nucleons with momenta in excess of 1000 MeV/c. This will improve our ability to study the structure of

nucleon correlations in nuclei. Direct comparisons of heavy nuclei to deuterium at large x will allow us to map out the strength of two-nucleon correlations in both light and heavy nuclei. These data will also be significantly more sensitive to the presence of multi-nucleon correlations. Just as the ratio of heavy nuclei to deuterium at $x > 1.5$ shows that the distribution in heavy nuclei is dominated by two-nucleon correlations, a similar ratio of heavy nuclei to ³He at $x > 2.5$ may provide the first experimental signature of three-nucleon correlations. Multi-nucleon correlations will also modify the Q^2 -dependence of the ratio to deuterium, due to the QCD-evolution of the structure function. Any additional strength at $x > 2$ coming from multi-nucleon correlations in heavy nuclei will be evolved down to lower x values as Q^2 increases, leading to an increase in the ratio to deuterium. Figure IV-5 shows calculations of this ratio with and without the presence of multi-nucleon correlations. E02-019 will reach $Q^2 \approx 8 \text{ GeV}^2$ for $x \approx 1.7$, where the multi-nucleon correlation model predicts a factor of two increase in this ratio. This will be an important first step in the study of multi-nucleon correlations.

In addition to probing nucleon distributions and short range correlations, these data fill in a significant void in our knowledge of the nuclear structure function. Little data exist for nuclei at large x , yet such data are important in the study of scaling and duality, higher twist effects, and nuclear dependence of the structure function. In addition, while the $x > 1$ structure function is often neglected, it must be included in studies of the energy-momentum sum rule or analysis of the QCD moments. While E02-019 will focus on the study of the high momentum nucleons in nuclei, it provides the data necessary for a variety of studies.

¹J. Arrington *et al.*, Phys. Rev. Lett. **82**, 2056 (1999).

²Jefferson Lab Experiment E02-019, 'Inclusive Scattering from Nuclei at $x > 1$ and High Q^2 with a 6 GeV Beam', J. Arrington, D. B. Day, A. Lung, and B. W. Filippone spokespersons.

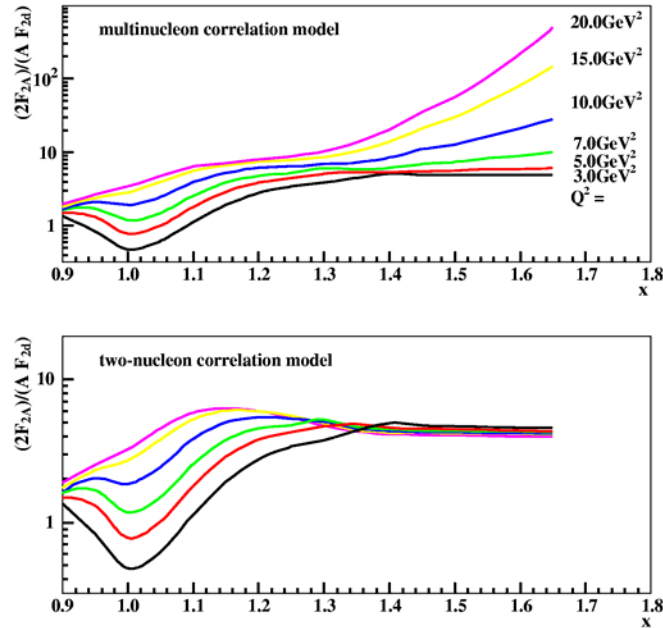


Fig. IV-5. Calculation of the ratio of structure function of Iron to Deuterium for $x > 1$ in the two-nucleon correlation model and the multi-nucleon correlation model.

C. QUARK STRUCTURE OF MATTER

c.1. The Structure Function of the Pion (R. J. Holt, P. E. Reimer, and K. Wijesooriya)

The light mesons have a central role in nucleon and in nuclear structure. The masses of the lightest hadrons, the mesons, are believed to arise from chiral symmetry breaking. The pion, being the lightest meson, is particularly interesting not only because of its importance in effective theories, but also because of its importance in explaining the quark sea in the nucleon and the nuclear force in nuclei. Most of our information about the pion structure function in the valence region originates from πp Drell-Yan scattering on a W target. The analysis of the Drell-Yan data was questioned¹ recently, and now studies of this analysis are underway. The Drell-Yan data² were re-analyzed with the following improvements: next-to-leading

order analysis, modern nucleon structure functions and modern nuclear effects, and a less-restrictive formula for the pion structure function. The results of this re-analysis are undergoing checks now to ensure reliability.

Studies were completed to examine the feasibility of making measurements at Jefferson Lab using an 11-GeV incident electron beam. With the relatively high luminosity which can be achieved at an upgraded Jefferson Lab, the pion structure can be measured, over a limited range in x . Additional investigations are being made of this reaction using a future electron-ion collider.³

¹M. B. Hecht *et al.*, Phys. Rev. C **63**, 025213 (2001).

²J. S. Conway *et al.*, Phys. Rev. D **39**, 92 (1989).

³R. J. Holt and P. E. Reimer, Proc. of the Second Workshop on the Polarized Electron Ion Collider, MIT (2000).

c.2. Measurements of Spin-Structure Functions and Semi-Inclusive Asymmetries for the Nucleon at HERA (H. E. Jackson, A. El Alaoui, K. G. Bailey, T. P. O'Connor, K. Hafidi, D. H. Potterveld, P. Reimer, Y. Sanjiev, and the HERMES Collaboration)

HERMES, HERA measurement of spin, is an international collaboration of 31 institutions formed to address a basic question of hadronic structure. How do the spins of its constituent quarks combine with the spin of the glue and the angular momentum of the partons to give the proton its spin of $\frac{1}{2}$? The HERMES experiment uses polarized internal targets in the HERA 30 GeV lepton storage ring at the DESY laboratory, in Hamburg Germany. By emphasizing semi-inclusive deep inelastic scattering (SIDIS) in which a hadron is observed in coincidence with the scattered lepton, HERMES brings a new dimension to studies of spin structure. The collaboration has collected and analyzed millions of deep-inelastic scattering events using longitudinally polarized electrons and positrons incident on longitudinally polarized internal gas targets of ^1H , ^2H , and ^3He , as well as thicker unpolarized gas targets. Measurements have been extended to a new domain during the past year with the installation and commissioning of a target with polarization transverse to the beam polarization. The scope of the HERMES program has evolved far beyond the original focus on the spin structure of the nucleon and now encompasses a broad range of subjects in polarized and unpolarized physics, but with the common goal of providing fundamental insights into the structure of the nucleon and how it is affected by the nuclear medium.

The study of the spin structure of the nucleon continues to be of highest priority. Spin asymmetries have been measured using polarized targets of hydrogen, deuterium, and ^3He . Analysis of the inclusive and semi-inclusive deep-inelastic scattering data from these unique undiluted targets has resulted in the world's most precise determination to date of the separate contributions of the up, down and sea quarks to the nucleon spin. Preliminary results from the most recent analyses have probed for the first time directly the polarization of the strange sea as well as the flavor asymmetry of the light sea polarization. While inclusive measurements have become a calibration benchmark for SIDIS studies, even here new physics continues to emerge. For the first time, the tensor polarized structure function for the deuteron has been measured using the HERMES polarized target. The result shows the promise of a new probe of nuclear effects at the partonic level. The observation of a single-spin asymmetry in the azimuthal distribution of positive pions detected in coincidence with the deep-inelastic scattering of positrons from a *longitudinally*

polarized proton target has been a development of major interest.

The theoretical interpretation of this result is under vigorous discussion. One possible explanation involves a particular chiral-odd fragmentation function that could make feasible at HERMES the first measurement of transversity, the only remaining unmeasured and one of the three most fundamental (leading twist) flavor-sets of parton distribution functions. Current measurements with a transversely polarized proton target will provide a clear test of the validity of this explanation as opposed to an alternative possible reaction mechanism, the Sivers effect, which involves totally different physics. Recent measurement of a lepton-beam spin asymmetry in the azimuthal distribution of detected photons in Deeply Virtual Compton Scattering (DVCS) has provoked wide interest. Interference with the indistinguishable but well-understood Bethe-Heitler process fortuitously gives rise to a rich variety of such asymmetries, which will continue to emerge from HERMES data. DVCS is considered to be the most reliable of the various hard exclusive processes that constrain the generalized or 'skewed' parton distributions, which are now the subject of intense theoretical development as, *e.g.*, they embody information about *orbital* angular momenta of partons. This type of measurement has been extended to exclusive and semi-inclusive electroproduction of pions and kaons where HERMES is releasing regularly new data showing for the first time substantial single-spin azimuthal asymmetries.

The ability to run with high density unpolarized targets provides HERMES with a tool reaching far beyond spin structure studies. The large momentum and solid angle acceptance of the HERMES spectrometer open a broad range of physics topics to exploration, and have resulted in a tool for the general study of photon-hadron interactions. Using its unique capabilities, in recent years HERMES has performed a measurement of the flavor asymmetry between up and down quarks in the nucleon sea, studies of fragmentation of up and down quarks to pions, measurement of the DIS and resonance contributions to the generalized Gerasimov-Drell-Hearn integral for both the proton and neutron, a measurement of the spin transfer from virtual photons to Λ^0 hyperons, and measurements of the effect of the nuclear environment. In the past year, a demonstration of the effects of color transparency in the production of rho mesons has been published, and the study of parton

propagation in nuclei has been extended to heavy nuclear targets. Recent developments and new results pertaining to these physics topics are discussed in more detail below.

The spectrometer and associated equipment continue to perform at design capability. As time and resources permit, systems are continually upgraded and new capabilities are added. The data acquisition software has been completely revamped to run under linux. The RICH particle identification system provides hadron separation over almost the full HERMES acceptance. A new transversely polarized target has been installed for operations during the 2002-2004 running period.

c.3. Flavor Decomposition of the Sea Quark Helicity Distributions in the Nucleon from Semi-Inclusive Deep-Inelastic Scattering (K. Hafidi, A. El Alaoui, K. G. Bailey, T. P. O'Connor, H. E. Jackson, D. H. Potterveld, P.E. Reimer, and the HERMES Collaboration)

The last decade has seen a remarkable progress in measuring the polarized quark distribution using inclusive Deep Inelastic Scattering (DIS). However, the information available from DIS has inherent limitations, as the cross sections are sensitive to only the square of the charge of the quark absorbing the exchanged virtual photon. Therefore sea quarks can not be distinguished from valence quarks. In addition the precision and kinematic coverage of the DIS measurements is still rather limited. Consequently, present Next to Leading Order (NLO) analyses also use information from hyperon β -decay to constrain the problem via the additional assumption of SU(3) flavor symmetry among baryons, which is known to be inexact. The results from QCD NLO analyses indicated that the quark spin account for a relatively small fraction of the total nucleon spin, of order of 20-40% (the value depends on the NLO factorization scheme used in the analysis). Further, the strange sea would seem to have a negative polarization of order of -10% which is very sensitive to SU(3) symmetry breaking effect.

Semi-inclusive measurements represent an alternative approach that avoids this assumption about SU(3) symmetry and allows direct measurements of the quark helicity distributions and in the particular of the sea quarks. In these measurements, a hadron is detected in coincidence with the scattered beam lepton. Through the fragmentation functions, a probabilistic relation exists between the flavor of the struck quark and the flavor content of the hadrons generated in the final state. By measuring the spin asymmetry for hadrons of

Installation of a system of silicon strip detectors for enhanced detection of Lambda decay products is almost complete. Design work is in progress for a large acceptance recoil detector array to be used to enhance solid angle acceptance and missing mass resolution in planned measurements of DVCS. These continuing investments in enhanced capability ensure that HERMES will continue to produce results at the forefront of the field. HERMES has a broad physics program and has had scientific impact on a number of fundamental questions about the strong interaction. HERMES is playing an important role in the worldwide experimental investigation of QCD.

various types, one may separate the polarized parton distributions by flavor.

Measurements of scattering asymmetries with identified pions and kaons from a deuterium target in combination with identified pions from hydrogen target and with inclusive data result in the first five flavor extraction of quark polarizations, *i.e.* Δu , Δd , $\Delta \bar{u}$, $\Delta \bar{d}$, and Δs from semi inclusive data, with the only assumption that s and \bar{s} have the same polarization. Factorization into parton distributions and fragmentation functions is assumed in the relation between the measured asymmetries and quark polarizations. The resulting coefficients or "purities" include effects of experimental acceptance, and are determined with a Monte Carlo generator and CTEQ low Q^2 parton distributions.

Figure IV-6a shows the results compared to two LO QCD fits¹ to previously published inclusive data. These fits not only assume SU(3) flavor symmetry to incorporate hyperon β -decay data, but also here invoke symmetry among the sea distributions in order to present them separately. The extracted helicity distributions of $u(x)$ and $d(x)$ are consistent with previous (semi) inclusive results.² The sea distributions, extracted separately here for the first time, are consistent with zero and with each other. There is no indication of the negative polarization of the strange sea that appears in the analysis of only inclusive data assuming SU(3) symmetry applied to hyperon β -decay data. Another interesting feature of the results, is shown in Fig. IV-6b, there is no evidence of a large a positive flavor asymmetry between $\bar{u}(x)$ and $\bar{d}(x)$ in

the light quark sea that was predicted by a theoretical calculation based on the chiral quark soliton model.³ In contrast to this possible discrepancy, this model does successfully explain the previously observed substantial value for the unpolarized flavor asymmetry between $\bar{u}(x)$ and $\bar{d}(x)$.⁴

In conclusion, a leading order extraction from new semi inclusive DIS data has produced separated helicity distributions for five flavors: Δu , Δd , $\Delta \bar{u}$, $\Delta \bar{d}$, and $\Delta s \equiv \Delta \bar{s}$. There is no evidence for either a negative strange sea polarization or for a flavor asymmetry in the helicity distributions of the light sea.

¹M. Glück *et al.*, Phys. Rev. D **63**, 094005 (2001); J. Blümlein and H. Bötcher *et al.*, Nucl. Phys. **B636**, 225 (2002).
²B. Adeva *et al.*, Phys. Lett. **B420**, 180 (1998); K. Ackerstaff *et al.*, Phys. Lett. **B464**, 123 (1999).
³B. Dressler *et al.*, EPJC **14**, 147 (2000).
⁴B. Dressler *et al.*, hep-ph/9809487.

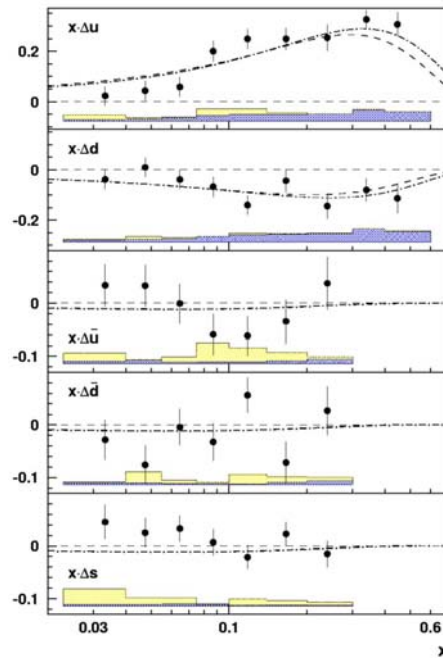


Fig. IV-6a. Quark helicity distributions at $\langle Q^2 \rangle = 2.5 \text{ GeV}^2$ as a function of Bjorken x .

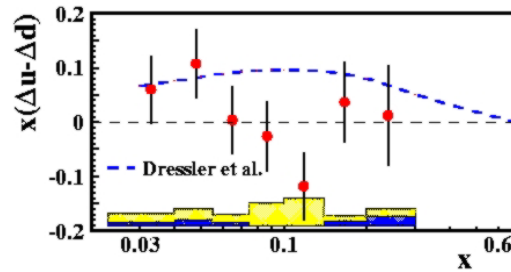


Fig. IV-6b. The light quark sea flavor asymmetry $\Delta \bar{u} - \Delta \bar{d}$ in the helicity distributions, at $\langle Q^2 \rangle = 2.5 \text{ GeV}^2$.

c.4. Study of Factorization and Flavor Content of the Nucleon in Unpolarized Semi Inclusive Deep Inelastic Scattering at HERMES (K. Hafidi, A. El Alaoui, K. G. Bailey, T. P. O'Connor, H. E. Jackson, D. H. Potterveld, P. E. Reimer, and the HERMES Collaboration)

Semi Inclusive Deep Inelastic Scattering (SIDIS) has been used extensively in recent years as an important testing ground for QCD. Indeed, SIDIS offers a great opportunity for studying the spin and the flavor content of the nucleon. However, using SIDIS relies on the factorization assumption between the hard scattering process and the hadronization of the struck quark.

Although at high energy the scattering and production mechanisms factorize, it remains unclear to what extent factorization applies at lower energies. HERMES has shown that within the experimental precision, which was dominated by statistical accuracy, factorization works reasonably well at the HERMES kinematic conditions.¹ By accumulating an order of magnitude more statistics, it is now possible to perform a more precise test of factorization.

In this analysis, all HERMES unpolarized and averaged polarized hydrogen and deuterium data have been used. The ratios $(\bar{d} - \bar{u})/(u - d)$ and d_v/u_v will be determined from the analysis of charged pion yields. The kinematic range is $0.02 < x < 0.4$ with the average Q^2 of 2.5 GeV^2 . The flavor asymmetry $(\bar{d} - \bar{u})/(u - d)$ was determined for fixed x -bins as a function of z , where z is the fraction of photon energy carried by the detected hadron. A flat z -dependence would be the proof of factorization. As shown in Fig.IV-7, the projected statistical precision of the ongoing analysis represents a considerable improvement of our ability to check factorization.

¹K. Ackerstaff *et al.*, Phys. Rev. Lett. **81**, 5519 (1998).

²E. A. Hawker *et al.*, Phys. Rev. Lett. **80**, 3715 (1998); R. S. Towell *et al.*, Phys. Rev. D **64**, 052002 (2001).

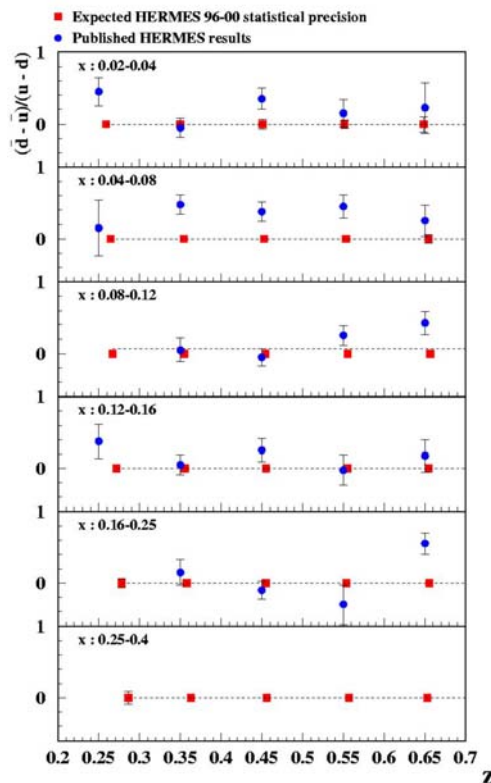


Fig. IV-7. The projected $(\bar{d} - \bar{u})/(u - d)$ as a function of z in different bins of x , compared with previously-published results.

The extraction of the sea flavor asymmetry and also the valence quark distribution in the proton will be performed. The measurement of the ratio \bar{d}/\bar{u} from Fermilab Drell-Yan experiment² E866 seems to indicate that at $x \sim 0.3$, the ratio begins to become smaller than unity which means that the sea asymmetry reverses from an excess of \bar{d} at low x to an excess of \bar{u} at high x . HERMES data can access the relatively high x region up to $x \sim 0.4$. Measuring d_v/u_v will provide an

additional test of factorization by comparing HERMES results with a QCD fit of other high energy data. In conclusion, with the ongoing analysis, we will be able to quantify with high precision the validity of the factorization assumption. We will also extract the flavor asymmetry ratio $(\bar{d} - \bar{u})/(u - d)$ and the valence content of the proton d_v/u_v using π^+/π^- yield ratios on hydrogen and deuterium.

c.5. Azimuthal Asymmetries and Transversity (H. E. Jackson, A. El Alaoui, K. G. Bailey, T. P. O'Connor, K. Hafidi, D. H. Potterveld, P. Reimer, Y. Sanjiev, and the HERMES Collaboration)

Recent measurements of single-spin azimuthal asymmetries by HERMES have been recognized as a potentially powerful source of information about the spin structure of the nucleon,¹ complementary to inclusive deep-inelastic scattering. Significant azimuthal target-spin asymmetries in electroproduction of charged and neutral pions on a longitudinally polarized hydrogen target has been published.^{2,3} It has been suggested that these single-spin asymmetries may provide information on the transversity distribution, which describes the probability to find a quark with its spin parallel or antiparallel to the spin of the nucleon that is polarized transversely to its infinite momentum. Transversity is a chiral-odd distribution function, which implies that it is not observable in an inclusive measurement. Therefore, a second chiral-odd object must be involved in the process to conserve chirality. In semi-inclusive scattering this has been postulated to be a chiral odd fragmentation function, the Collins function. The HERMES results on target single-spin asymmetries have elicited a number of phenomenological studies to evaluate these asymmetries in the framework of the Collins mechanism. Theoretical predictions have also been made for single-spin asymmetries in DIS off the nucleons in a deuterium target.

kaon production on a longitudinally polarized deuterium target. The data were recorded during the 1998, 1999, and 2000 running period of the HERMES experiment. The measured asymmetries show no dependence on polarity of the beam charge. The requirements imposed on the kinematics of the scattered lepton are $1 \text{ GeV}^2 < Q^2 < 15 \text{ GeV}^2$, $W > 2 \text{ GeV}$, $0.023 < x < 0.4$ and $y < 0.85$. Contributions from target fragmentation are suppressed by requiring $z > 0.2$ and exclusive meson production is suppressed by requiring the cut $z < 0.7$. The asymmetries appear in the distribution of the hadrons in the azimuthal angle ϕ around the virtual photon direction, relative to the lepton scattering plane. In Fig. IV-8, the azimuthal asymmetries are displayed as a function of ϕ , integrated over the experimental acceptance. The corresponding analyzing powers in the $\sin \phi$ moment of the cross section are $0.012 \pm 0.002(\text{stat}) \pm 0.002(\text{syst.})$ for positive pions, $0.006 \pm 0.003(\text{stat}) \pm 0.002(\text{syst.})$ for negative pions, $0.021 \pm 0.005(\text{stat}) \pm 0.003(\text{syst.})$ for neutral pions, and $0.013 \pm 0.006(\text{stat}) \pm 0.003(\text{syst.})$ for positive kaons. These findings can be well described by model calculations where the asymmetries are interpreted in the context of transversity. The observed asymmetries for positive pions and kaons are consistent with the assumption of u-quark dominance in the quark distribution and fragmentation process.

HERMES has made the first observation of target-spin azimuthal asymmetries for semi-inclusive pion and

¹P. J. Mulders and R. D. Tangermann, Nucl. Phys. B **461**, 197 (1996).

²HERMES collaboration, A. Airapetian *et al.*, Phys. Rev. Lett. **84**, 4047 (2000).

³HERMES collaboration, A. Airapetian *et al.*, Phys. Rev. **64**, 097101 (2001).

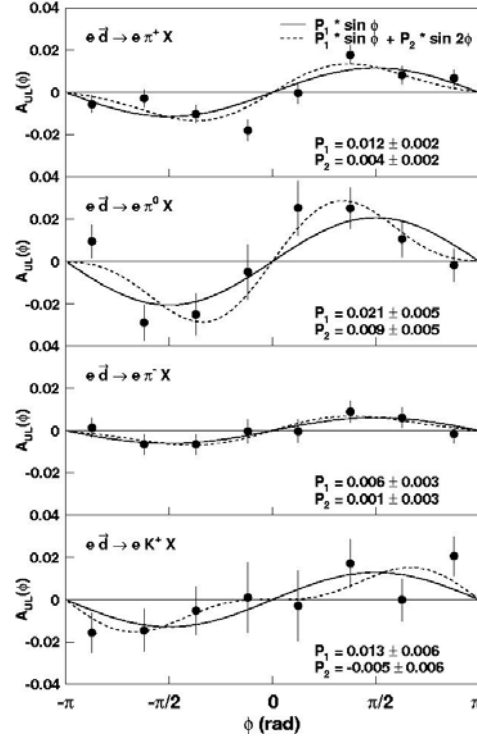


Fig. IV-8. Target spin asymmetries $A_{UL}(\phi)$ for electroproduction of π^+ , π^0 , π^- and K^+ mesons. Fits of the form $P_0 + P_1 \sin \phi$ (solid line) and $P_0 + P_1 \sin \phi + P_2 \sin 2\phi$ (dashed line) are also displayed in the figure. The error bars give the statistical uncertainties of the measurements. The values of the coefficients P_0 are all compatible with zero and the coefficients P_1 and P_2 for the various hadrons and their statistical uncertainties are listed in each panel.

c.6. Evidence for Quark-Hadron Duality in the Proton Spin Asymmetry A_1

(H. E. Jackson, A. El Alaloui, K. G. Bailey, T. P. O'Connor, K. Hafidi, D. H. Potterveld, P. Reimer, and the HERMES Collaboration)

The interaction between baryons and between baryons and leptons can generally be described by two complementary approaches: with quark-gluon degrees of freedom at high energy, where the quarks are asymptotically free, and in terms of hadronic degrees of freedom at low energy, where effects of confinement are large. In some specific cases, where the description in terms of hadrons is expected to apply most naturally, the quark-gluon description can be successfully used. Such cases are examples of so-called quark-hadron duality. Bloom and Gilman¹ first noted this relationship between phenomena in the nucleon resonance region and in deep inelastic scattering (DIS). Specifically, they observed that the cross section for electro-production of nucleon resonances, if averaged over a large enough range of invariant mass W of the initial photon-nucleon system, exhibited the same

behavior as the cross section observed in the DIS region. In other words, the curve measured as a function of the Bjorken scaling variable $x = Q^2/2m\nu$ in DIS processes at high Q^2 and high ν , approximately approaches the averaged curve measured in the resonance region at lower ν and Q^2 (here $-Q^2$ is the transferred four-momentum squared, M is the proton mass and ν the energy of the exchanged virtual photon in the target rest frame). The spin-dependent lepton-nucleon scattering data taken by HERMES have been used to investigate the validity of the concept of quark-duality for the spin asymmetry A_1 . Longitudinally polarized positrons were scattered off a longitudinally polarized hydrogen target for values of Q^2 between 1.2 and 12 GeV^2 and values of W^2 between 1 and 4 GeV^2 .

¹E. D. Bloom and F. J. Gilman, Phys. Rev. **D4**, 2901 (1971).

²A. Airapetian *et al.*, Phys. Rev. Lett. **90**, 052501 (2003).

The average double-spin asymmetry in the nucleon resonance region is found to agree² with that measured in DIS at the same values of the Bjorken scaling variable x . This finding implies that the description of

A_1 in terms of quark degrees of freedom is valid in the nucleon resonance region for values of Q^2 above 1.6 GeV².

c.7. Search for the Onset of Color Transparency: The JLab E02-110 Experiment

(K. Hafidi, B. Mustapha, J. Arrington, A. El Alaoui, D. F. Geesaman, R. J. Holt, D. H. Potterveld, P. E. Reimer, E. C. Schulte, X. Zheng, and the Hall B Collaboration)

According to QCD, pointlike colorless systems, such as those produced in exclusive processes at high Q^2 have a vanishingly small transverse size. Therefore, they are expected to travel through nuclear matter experiencing very little attenuation. This phenomenon is known as color transparency (CT). An analogous mechanism is well known in QED: the interaction cross section of an electric dipole is proportional to its square size. As a result the cross section vanishes for objects with very small electric dipole moments. Since color is the charge of QCD, and by analogy to QED, the cross section of a color-neutral dipole, as formed by a pair of oppositely colored quarks for instance, is also predicted to vanish for small sized hadrons. Color transparency cannot be explained in the hadronic picture of nuclear matter (Glauber theory) and calls upon the quark's degrees of freedom. Earlier measurements were mainly focused on quasi-elastic hadronic ($p,2p$)¹ and leptonic ($e,e'p$)² scattering off nuclear targets. None of these experiments were able to produce evidence for CT up to $Q^2 \sim 8$ GeV². The strongest evidence for CT so far comes from Fermilab experiment E791 on the A-dependence of coherent diffractive dissociation of 500 GeV/c pions into di-jets.³ A recent measurement performed by the HERMES collaboration using exclusive ρ^0 electroproduction off nitrogen adds further evidence for the existence of CT.⁴

The main goal of E02-110 experiment⁵ is to look for the onset of CT in the incoherent diffractive ρ^0 electro and photoproduction on deuterium, carbon and copper. In this process (see Fig. IV-9a), the virtual photon fluctuates into $q\bar{q}$ pair which travels through the nuclear medium evolving from its small initial state

with a transverse size proportional to $1/Q$, to a "normal size" vector meson detected in the final state. Therefore, by increasing the value of Q^2 one can squeeze the size of the produced $q\bar{q}$ wave packet. The photon fluctuation can propagate over a distance which is known as the coherence length ℓ_c . The coherence length can be estimated relying on the uncertainty principle and Lorentz time dilatation as $\ell_c = 2\nu/(Q^2 + M_{q\bar{q}}^2)$, where ν is the energy of the virtual photon and $M_{q\bar{q}}$ is the mass of the $q\bar{q}$ pair dominated by the ρ^0 mass in the case of exclusive ρ^0 electroproduction. What is measured in the reaction is how transparent the nucleus appears to "small size" ρ^0 by taking the ratio of the nuclear per-nucleon (σ_A/A) to the free nucleon (σ_N) cross sections, which is called nuclear transparency $T_A = \frac{\sigma_A}{A\sigma_N}$. Consequently, the signature of CT is an

increase in the nuclear transparency T_A with increasing hardness (Q^2) of the reaction. Recent theoretical calculations by Kopeliovich *et al.*⁶ predicted an increase of more than 40% at $Q^2 \sim 4$ GeV².

However, one should be careful about other effects that can imitate this signal. Indeed, measurements by HERMES have shown that T_A increases when ℓ_c varies from long to short compared to the size of the nucleus. This so-called coherence length effect can mock the signal of CT and should be under control to avoid mixing it with CT effect.

¹A. S. Carroll *et al.*, Phys. Rev. Lett. **61**, 1698 (1988); Y. Mardor *et al.*, Phys. Rev. Lett. **81**, 5085 (1998); A. Leksanov *et al.* Phys. Rev. Lett. **87**, 212301 (2001).

²N. C. R. Makins *et al.*, Phys. Rev. Lett. **72**, 1986 (1994); T. G. O'Neill *et al.*, Phys. Lett. **B351**, 87 (1995); D. Abbott *et al.*, Phys. Rev. Lett. **80**, 5072 (1998); K. Garrow *et al.*, Phys. Rev. C **66**, 044613 (2002).

³E. M. Aitala *et al.*, Phys. Rev. Lett. **86**, 4773 (2001).

⁴A. Airapetian *et al.*, Phys. Rev. Lett. **90**, 052501 (2003).

⁵Jefferson Lab Experiment E02-110, "Q² Dependence of Nuclear Transparency for Incoherent ρ^0 electroproduction", K. Hafidi, B. Mustapha and M. Holtrop spokespersons.

⁶B. Kopeliovich *et al.*, Phys. Rev. C **65**, 035201 (2002).

Therefore, the E02-110 experiment will measure the Q^2 dependence of the transparency T_A at fixed coherence length ℓ_c . Figure IV-9b shows the projected uncertainties for complementary ℓ_c values to map the

whole Q^2 region up to 4 GeV^2 . These measurements will benefit from the high luminosity beam available at JLab and the large acceptance spectrometer (CLAS) in Hall B.

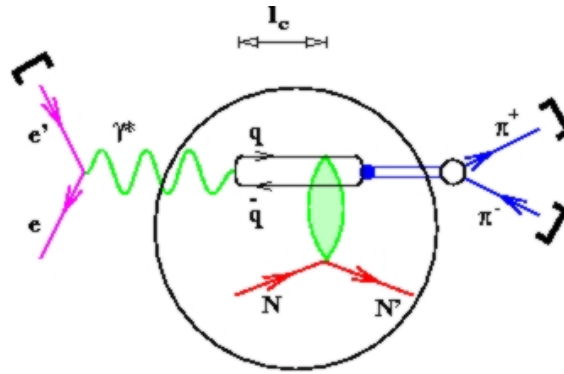


Fig. IV-9a. Exclusive lepton production of the ρ^0 meson.

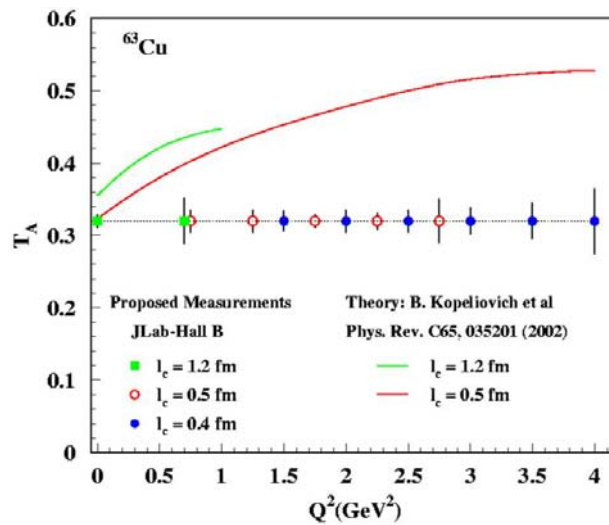


Fig. IV-9b. Theoretical predictions and expected statistical accuracy

c.8. The Q^2 Dependence of Nuclear Transparency for Exclusive ρ^0 Production

(K. Hafidi, A. El Alaoui, K. G. Bailey, T. P. O'Connor, H. E. Jackson, D. H. Potterveld, P. E. Reimer, and the HERMES Collaboration)

One of the fundamental predictions of QCD is the existence of a phenomenon called Color Transparency (CT). With the same goal and spirit of the measurements in the previous report,* HERMES measured the nuclear transparency for exclusive ρ^0 electroproduction on hydrogen and nitrogen and for fixed coherence length values ℓ_c covering the region from 1.3 to 2.5 fm. Presenting the data in a way which

keeps ℓ_c constant represents a simple prescription to eliminate the Coherence Length (CL) effect from the Q^2 dependence of the nuclear transparency. A value for T_A has been extracted for each (ℓ_c, Q^2) sub-bin for ρ^0 production (as illustrated in Fig. IV-10 for coherent production on nitrogen). The data have been fitted with a common Q^2 slope (p_1), which has been extracted assuming $T_A = p_0 + p_1 \cdot Q^2$. Combining both coherent

and incoherent production, the value of the Q^2 slope was found to be positive and equal to (0.074 ± 0.021) GeV^{-2} .¹ This result represents a more than a 3σ signal of Color Transparency, and is in good agreement with

the theoretical predictions.² It represents one of the very few measurements that can claim to provide evidence of Color Transparency.

¹A. Airapetian *et al.*, Phys. Rev. Lett. **90**, 052501 (2003).

²B. Kopeliovich *et al.*, Phys. Rev. C **65**, 035201 (2002) 035201.

*Footnote: see previous report on "Search for the Onset of Color Transparency: The JLab E02-110 Experiment".

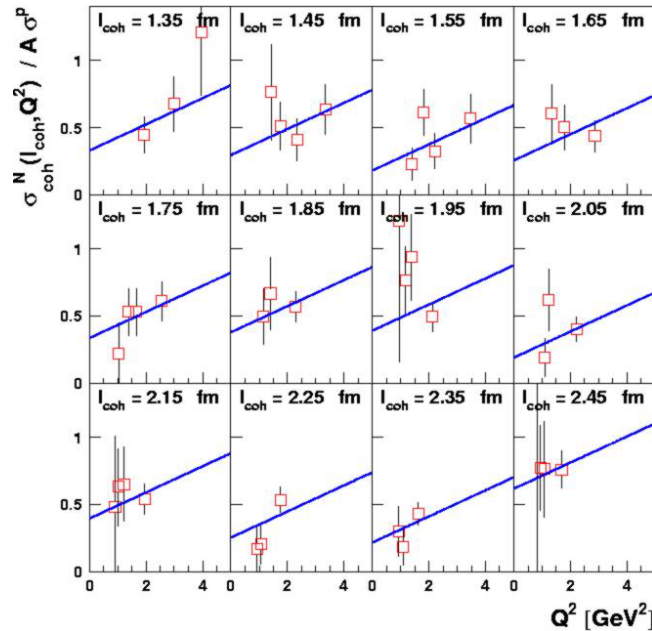


Fig. IV-10. Nuclear transparency as a function of Q^2 in fixed l_c bins for coherent ρ^0 electroproduction on nitrogen.

c.9. The Q^2 Dependence of the Generalized Gerasimov-Drell-Hearn Integral for the Deuteron, Proton, and Neutron (H. E. Jackson, A. El Alaloui, K. G. Bailey, T. P. O'Connor, K. Hafidi, D. H. Potterveld, P. Reimer, and the HERMES Collaboration)

The Gerasimov-Drell-Hearn (GDH) sum rule connects the anomalous contribution to the magnetic moment of the target nucleus with an energy-weighted integral of the difference of the helicity-dependent photoabsorption cross sections. Originally conceived for real photons, the GDH integral can be generalized to the case of photons with virtuality Q^2 . For spin $1/2$ targets such as the nucleon, it then represents the non-perturbative limit of the first moment Γ_1 of the spin structure function $g_1(x, Q^2)$ in deep inelastic scattering (DIS). The data collected by HERMES with a deuterium target have been analyzed together with a re-analysis of previous measurements on the proton. These data provide an unprecedented and complete measurement of the generalized GDH integral for photon-virtuality ranging over $1.2 < Q^2 < 12.0 \text{ GeV}^2$

and for photon-nucleon invariant mass squared W^2 ranging over $1 < W^2 < 45 \text{ GeV}^2$, thus covering simultaneously the nucleon-resonance and the deep inelastic scattering regions. These data allow the study of the Q^2 dependence of the full integral, which is sensitive to both the Q^2 -evolution of the resonance form factors and contributions of higher twist. The contribution of the nucleon-resonance region is seen to decrease rapidly with increasing Q^2 . As expected, at higher Q^2 the data are found to be in agreement with previous measurements of the first moment of g_1 . From data on the deuteron and proton, the GDH integral for the neutron has been derived and the proton-neutron difference evaluated. This difference is found to satisfy the fundamental Bjorken sum rule at $Q^2 = 5 \text{ GeV}^2$

c.10. First Measurement of the Deuteron Tensor Polarized Structure Function b_1

(H. E. Jackson, A. El Alaoui, K. G. Bailey, T. P. O'Connor, K. Hafidi, D. H. Potterveld, P. E. Reimer, Y. Sanjiev, and the HERMES Collaboration)

The deep inelastic scattering (DIS) of leptons by nucleons is characterized by four fundamental structure functions, F_1 , F_2 , g_1 , and g_2 . The latter two require polarized beams and targets in order to be measured, and the study of g_1 has been a primary goal for HERMES. When a deuteron is the scatterer, there are four additional fundamental structure functions,¹ b_{1-4} , that arise because the deuteron has spin 1, but which have never before been measured. The first, b_1 , is of considerable interest. It is sensitive to differences in the quark momentum distribution between the 0 helicity (q^0) and the spin-averaged ± 1 helicity ($q^+ + q^-$) states of the hadron. Of leading twist, b_1 should be identically zero for a simple composition of nucleons in the s state. However, a non-zero b_1 is possible through nuclear effects such as binding, the d state of the deuteron, and shadowing effects such as coherent double scattering.^{2,3} If non-zero, it should properly be taken into account when extracting the neutron structure functions from deuterium data (hitherto it has been ignored.) Moreover, a non-zero value could indicate that the

quark sea becomes tensor polarized in the deuteron, which is unexpected in the naïve quark parton model.

HERMES has measured b_1 for the first time, using the same gaseous, tensor-polarized deuterium target developed for its nucleon structure function measurements⁴. An atomic beam source injected deuterium atoms of specific nuclear polarization states into a windowless storage cell in the HERA positron ring, and scattered particles were detected and identified in the HERMES detector. The tensor asymmetry of the DIS cross section, A_{zz} , is given by: $A_{zz} = [(\sigma^+ + \sigma^-) - 2\sigma^0]/(3\sigma_u T) \approx -2b_1/(3F_1)$, where σ^0 , σ^+ , and σ^- are the cross sections measured in the zero helicity and ± 1 helicity target states, σ_u is the unpolarized cross section, and T is the degree of tensor polarization in the target. The measured tensor asymmetry and inferred b_1 are shown as a function of the Bjorken variable x in Fig. IV-11.

¹P. Hoodbhoy *et al.*, Nucl. Phys. B **312**, 571 (1989).

²J. Edelmann *et al.*, Phys. Rev. C **57**, 3392 (1998).

³K. Bora and R.L. Jaffe, Phys. Rev. D **57**, 6906 (1998).

⁴K. Ackersdtaff *et al.*, Nucl. Instr. Meth. A **417**, 230 (1998).

⁵F. E. Close *et al.*, Phys. Rev. D **42**, 2377 (1990).

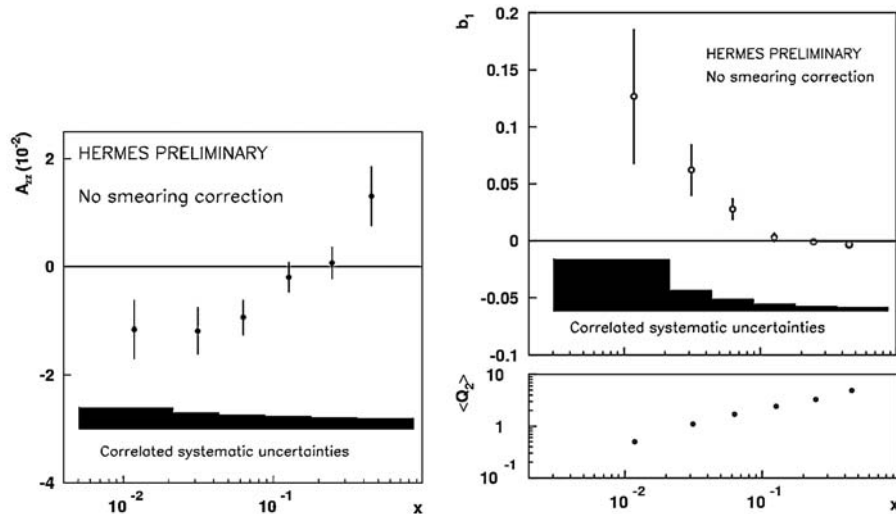


Fig. IV-11. Preliminary HERMES results for the tensor asymmetry A_{zz} (left plot) and b_1 (right plot) as a function of Bjorken x . The error bars are statistical only, and the shaded bands show the estimated systematic uncertainties. The Q^2 range of the measurements is shown in the lower panel on the right, in GeV^2 .

A_{zz} is found to be less than 0.02 over the measured range, and therefore its neglect in extracting g_1 from HERMES deuterium data is estimated to cause less than a 1% error. The data indicate that b_1 is small but different from zero, with a rise at low x that is

qualitatively consistent with models of coherent double scattering, suggesting a significant tensor polarization of the sea quarks that would violate the Close-Kumano sum rule.⁵ Further calculations of b_1 by the theoretical community are eagerly anticipated.

c.11. Measurements with Unpolarized Targets: Hadron Formation (H. E. Jackson, A. El Alaoui, K. G. Bailey, T. P. O'Connor, K. Hafidi, D. H. Potterveld, P. E. Reimer, Y. Sanjiev, and the HERMES Collaboration)

HERMES has an active program of measurements with unpolarized nuclear targets. By comparing the same interaction on different nuclear targets, HERMES is able to measure the effects of the nuclear medium on the interaction and subsequent hadronization of the quarks from the interaction. HERMES has measured the pion, kaon and (anti)proton fragmentation functions, and their attenuation in a nuclear environment. By embedding the fragmentation process in the nuclear medium, one can study the time propagation of the hadron formation process. In HERMES this attenuation is measured by the hadron multiplicity ratio, which is the ratio of the number of hadrons produced in a DIS event for on nuclear target to that from a deuterium target. The multiplicity ratio is measured as a function of the energy transferred to the struck quark, ν , and hadron energy fraction, $z = E_h/\nu$ (where E_h is the hadron's energy).

Hadron attenuation can be related to the formation length (or time) of the hadron. Such data can also be used to derive empirical values for the hadron formation time and the energy loss of a quark propagating in the medium. These quantities are of considerable theoretical and experimental interest, since these concepts also apply to the Drell-Yan process and heavy-ion collisions. HERMES data have been interpreted¹ in terms of final state interactions. This medium modification of the fragmentation of the propagating parton results from induced gluon radiation due to multiple parton scattering, and gives rise to additional terms in the QCD evolution equations that soften the fragmentation functions. As shown in Fig. IV-12, this treatment provides an excellent description of the HERMES results. From these data, this treatment gives a quark energy loss of $dE/dx \approx 0.5$ GeV/fm in cold nuclear matter.

¹E. Wang, and X.-N. Wang, Phys. Rev. Lett. **89** 162301 (2002).

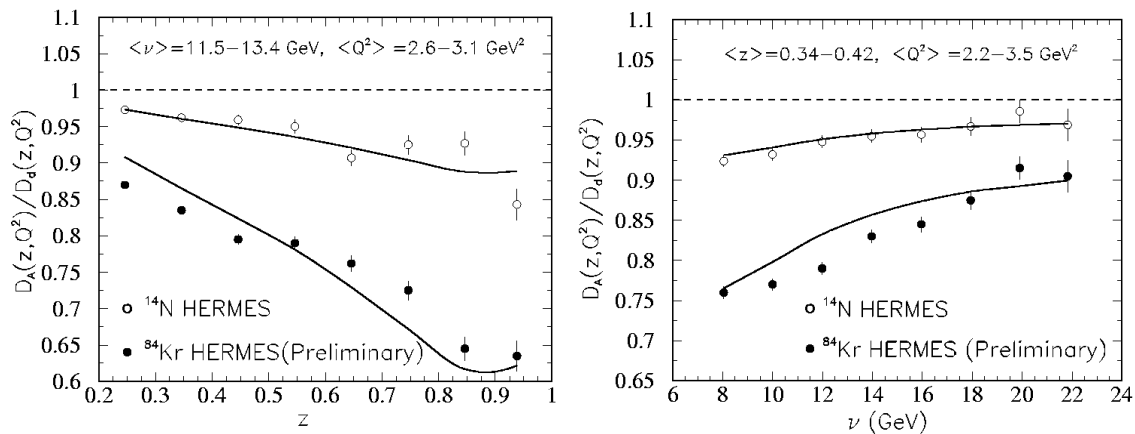


Fig. IV-12. At the left is the predicted nuclear modification of jet fragmentation functions (curves) compared to HERMES data on the ratios of hadron distributions between nuclear and deuterium targets in DIS. At the right is the energy dependence of this predicted nuclear modification (curves) compared to the HERMES data.

c.12. A Dual Radiator Ring-Imaging Cerenkov Counter for HERMES (H. E. Jackson, A. El Alaloui, K. G. Bailey, T. P. O'Connor, K. Hafidi, D. H. Potterveld, P. Reimer, and the HERMES Collaboration)

A dual radiator Ring Imaging Cerenkov (RICH) detector for the identification of hadrons has been in routine operation¹ as part of the HERMES spectrometer since 1998. Its design and construction which involved eight collaborating institutions was led by the Argonne group. The pattern recognition software for identification of the different hadrons in the RICH is based on two different methods: an indirect ray tracing method (IRT) and a direct ray tracing method (DRT). Both methods are combined in a likelihood analysis which selects the most probable particle type. The IRT and DRT exist in parallel; a decision network chooses the optimal method depending on event topology. The IRT method has been demonstrated to give reliable results, and has been the basis of all data analysis carried out to date. Features of the performance of the DRT method are not understood. Over most of the

range of momenta, contrary to expectation, DRT identification efficiencies are substantially lower than those of IRT. Work continues to understand this behavior, to test and to tune the DRT method. With the demonstration of reliable operation of DRT, a final training of the decision network will be performed in order to implement its use in providing the highest efficiencies for reliable particle identification. The particle samples obtained with these procedures will be characterized by efficiencies for correct identification of specific particle type and contamination of samples from mis-identification. Unfolding procedures have been developed for correcting for these effects. Current efforts are focused on developing analysis routines for propagating systematic errors in the parameters used in the unfolding procedure.

¹N. Akopov *et al.*, Nucl. Instr. Meth. **A479**, 511 (2002).

c.13. Measurement of the Antiquark Flavor Asymmetry of the Proton Sea Using Drell-Yan Scattering (P. E. Reimer, D. F. Geesaman, S. B. Kaufman, and the FNAL E866/NuSea collaboration)

While it is not required by any fundamental symmetry, it has—until recently—been widely assumed that the distributions of anti-down, \bar{d} , and anti-up, \bar{u} , quarks in the proton were identical. This was based on the assumption that the proton's sea arose perturbatively from gluons splitting into quark-antiquark pairs. Since the mass difference between the up and down quarks is small, equal numbers of up and down pairs would result. A ratio of \bar{d}/\bar{u} which is not unity is then a clear sign of nonperturbative origins to the quark-antiquark sea of the proton.

To explore the difference between \bar{d} and \bar{u} , Fermilab E866/NuSea measured the ratio \bar{d}/\bar{u} as a function of the momentum carried by the struck quark, x . This was accomplished using the Drell-Yan mechanism, in which

a quark (or antiquark) in the proton beam annihilates with an antiquark (or quark) in the target. The resulting annihilation produces a virtual photon that decays into a pair of leptons, which are seen in the detector. From the ratio of hydrogen to deuterium Drell-Yan cross sections, the ratio \bar{d}/\bar{u} and difference $\bar{d}-\bar{u}$ were extracted and unexpectedly large x -dependent flavor asymmetry in the proton's sea was revealed. The differences seen in Fig. IV-13 are non-perturbative in nature, and several approaches have been suggested that could produce this difference. These are represented by the curves in Fig. IV-13. These approaches include meson cloud models of the nucleon,¹ chiral quark models in which the mesons couple directly to the constituent quarks² and instanton models.³

¹J. C. Peng *et al.*, Phys. Rev. D **58**, 092004 (1998); N. Nikoleav *et al.*, Phys. Rev. D **60**, 014004 (1999).

²A. Szczurek *et al.*, J. Phys. G **22**, 1741 (1996); P.V. Pobylitsa *et al.*, Phys. Rev. D **59**, 034024 (1999).

³A. E. Dorokhov and N. I. Kochelev, Phys. Lett. B, 335 (1991); Phys. Lett. B **304** 167 (1993).

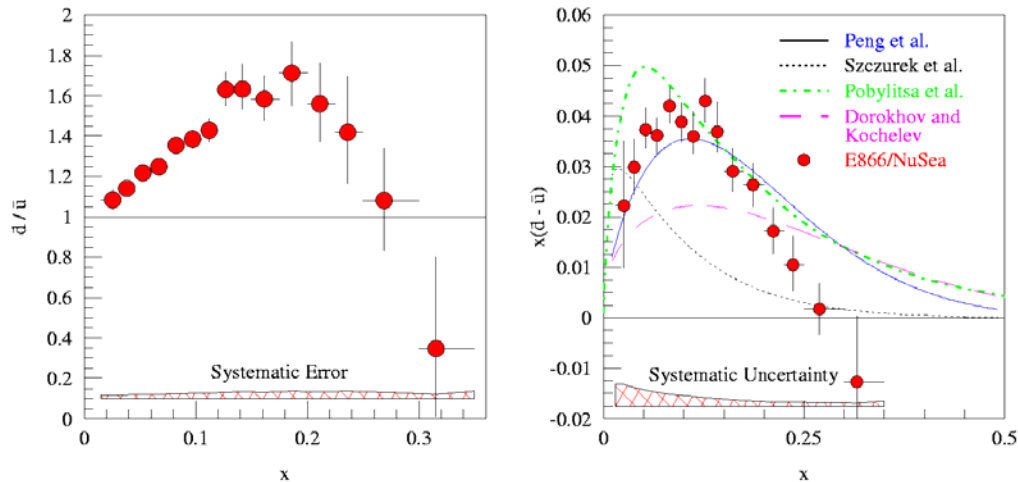


Fig. IV-13. The ratio of \bar{d}/\bar{u} (left) and $x(\bar{d}-\bar{u})$ (right) as a function of x , the fraction of the proton's momenta carried by the struck quark. The curves in the right graph represent different model calculations as described in the text.

c.14. Measurement of the Absolute Drell-Yan Cross Section on Hydrogen and Deuterium
 (P. E. Reimer, D. F. Geesaman, S. B. Kaufman, and the FNAL E866/NuSea Collaboration)

Very little is known about the regime in which only one parton carries much of proton's momentum—different theoretical treatments prescribe different behaviors as $x \rightarrow 1$ and very little data are available to serve as a guide. Drell-Yan absolute cross sections are sensitive to the high- x behavior of the *beam's* quarks and the intermediate- x behavior of the target antiquarks. E866 has measured the absolute cross sections for *proton-*

proton and *proton-deuterium* Drell-Yan. The Drell-Yan cross section is dominated by the beam proton distribution of $4u(x)+d(x)$ as $x \rightarrow 1$. The absolute cross sections, relative to a next-to-leading order (NLO) calculation are shown in Fig. IV-14. As can be seen in the figure, the quark distribution used in the calculation *overpredict* the data significantly at large- x .

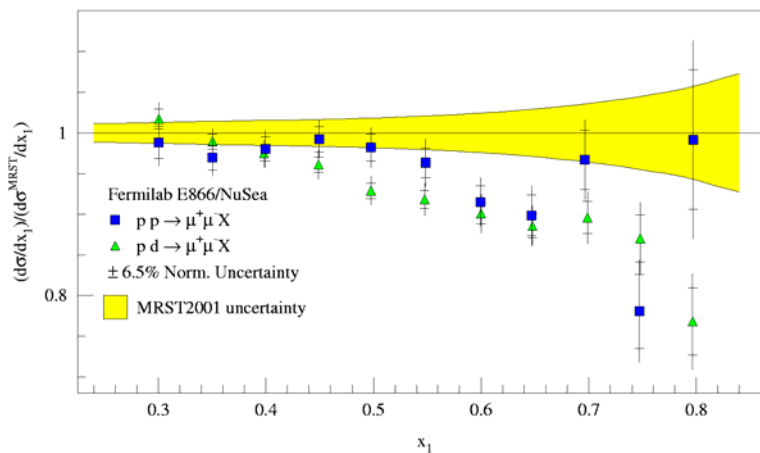


Fig. IV-14. The ratio of Drell-Yan cross section measured by Fermilab E866/NuSea for proton-deuterium (triangles) and proton-proton (squares) to calculated NLO cross section based on the MRST2001 parton distributions. The yellow band represents the uncertainty given by MRST2001 on $4u(x)+d(x)$.

c.15. Production of Υ and J/ψ from 800-GeV Protons Incident on Hydrogen and Deuterium (P. E. Reimer, D. F. Geesaman, S. B. Kaufman, and the FNAL E866/NuSea Collaboration)

The Υ and J/ψ mesons are produced when partons from the beam and target interact to form a virtual gluon, which then hadronizes into a heavy meson resonance. The virtual gluon may be generated by the annihilation of either a quark-antiquark pair or a pair of gluons (also called gluon-gluon fusion). Hence resonance production is sensitive to both the quark and gluon distributions with the target and beam. The J/ψ is believed to be produced primarily through gluon-gluon fusion, while Υ production is thought to proceed via both gluon-gluon fusion and quark-antiquark annihilation. Because the gluon distribution for the proton and neutron are similar, the per nucleon J/ψ cross section should be the same for both hydrogen and deuterium. For the Υ , on the other hand, the ratio of deuterium to hydrogen cross sections is expected to be larger than unity for the values of fractional momenta, x , probed by FNAL E866/NuSea, since $\bar{u}_n > \bar{u}_p$ in this region, which allows for more $u_{\text{beam}} \bar{u}_{\text{target}}$ annihilations with deuterium.

The FNAL E866/NuSea hydrogen and deuterium data contain 30 thousand Υ and 1 million J/ψ events. The production cross sections for these mesons have been extracted and can be compared to predictions based on models and parton distributions available in the literature. Color evaporation model calculations have been performed for both Υ and J/ψ production from hydrogen and deuterium. Although it is an extremely simple model, the color evaporation model does reproduce the observed x-Feynman shape of the cross section. The measured cross section ratios for both the J/ψ and the Υ are near unity as shown in Fig.IV-15. In the case of the J/ψ , this is not surprising, since J/ψ production is expected to proceed through gluon fusion. In the case of the Υ , however, the value near unity is in disagreement with color evaporation model calculations. This deviation may indicate that the parton distribution functions underestimate the hard gluon ($x \approx 0.25$) distribution in the proton.

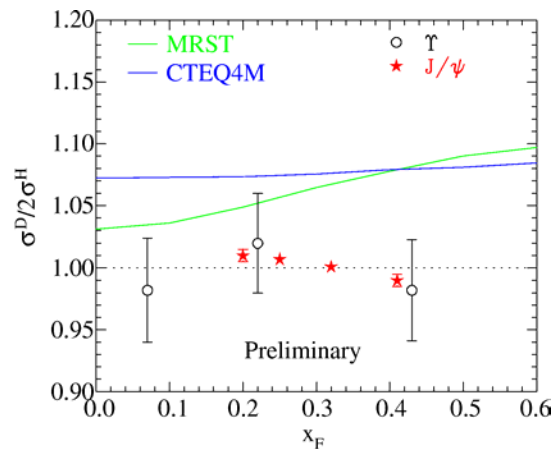


Fig. IV-15. The data points show the ratio of cross section for J/ψ and Υ production from deuterium to hydrogen. The curves represent color evaporation model calculations for this ratio for Υ production using two different parameterizations of the nucleon parton distributions. (J/ψ production is expected to have a ratio near 1.)

c.16. Drell-Yan Measurements with 120-GeV Protons, FNAL E906 (P. E. Reimer, D. F. Geesaman, J. Arrington, K. Hafidi, R. J. Holt, D. H. Potterveld, and the FNAL E906 Collaboration)

The Drell-Yan measurements of Fermilab E866/NuSea have provided new insight into the antiquark sea in the proton and nuclear dependence phenomena. FNAL E906 has been approved by Fermilab to extend Drell-Yan measurements to larger values of x (the fraction of the proton's momenta carried by the struck quark) using the new 120 GeV Main Injector at Fermilab.

The proton and the neutron are composite objects, made of quarks, antiquarks and gluons, collectively known as partons. While many of the properties of the proton may be attributed to its three valence quarks, it is, in fact, much more complicated, with over 50% of its momentum being carried by the its sea quarks and gluons. To understand the structure of the proton, it is necessary to understand the sea quarks, their origins and their interactions with the gluons that bind the proton together. E906 is specifically designed to probe the sea quarks of the proton. Vacuum polarization accounts for the creation of a flavor symmetric sea. Previous E866 Drell-Yan data, however, exhibit a large

asymmetry between \bar{d} and \bar{u} for $x < 0.25$ clearly indicating a non-perturbative origin to the sea. Above $x > 0.28$, however, the existing data, albeit with poor statistical uncertainty, indicate the ratio \bar{d}/\bar{u} returns to unity. This result dramatically changed the sea quark parton distribution fits and was completely unpredicted by meson cloud and other non-perturbative models.

The return of \bar{d}/\bar{u} to unity clearly signals a change in the mechanism by which the sea is generated. Fermilab E906 will determine \bar{d}/\bar{u} and $\bar{d}-\bar{u}$ for $0.1 \leq x \leq 0.45$, encompassing the non-perturbative region and extending well into the region where the sea appears to return to symmetry, allowing for the study of the relative importance of the perturbative and non-perturbative sea. The current parton distributions now reproduce the previous Drell-Yan data for $0.28 < x < 0.3$, but allow $\bar{d}/\bar{u} < 1$ as x increases above 0.3. This is not expected in either meson or perturbative models and is simply indicative of the complete lack of data. E906 will provide this data, as shown in Fig. IV-16.

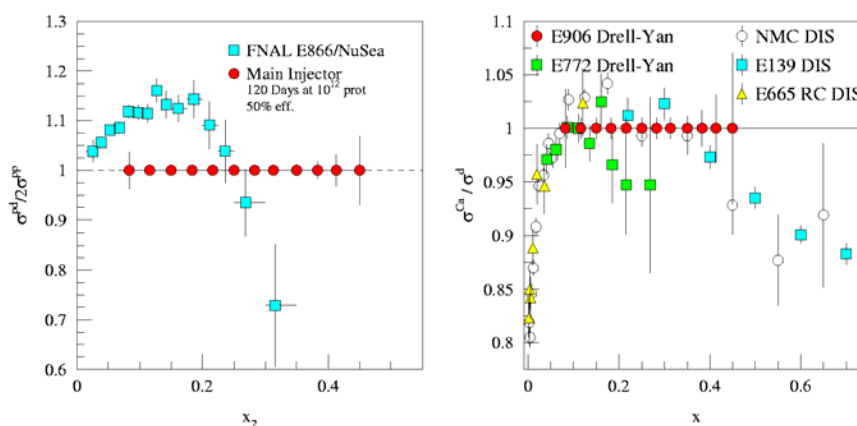


Fig. IV-16. The statistical uncertainty of E906's measurement of the ratio of hydrogen to deuterium cross sections (arbitrarily plotted at 1) compared with the E866 measurements of the same quantity (left). The statistical uncertainty of E906's measurement of the ratio of deuterium to calcium cross sections (arbitrarily plotted at 1) compared with previous Drell-Yan and deep inelastic scattering (DIS) measurements (right).

Very little is known about the regime in which only one parton carries much of proton's momentum—different theoretical treatments prescribe different behaviors as $x \rightarrow 1$ and very little data is available to serve as a guide. Through the partons in the beam proton, Fermilab E906 will access these distributions. The Drell-Yan cross section is dominated by the distribution of $4u(x)+d(x)$ as $x \rightarrow 1$. E906 will extend the data provided by

Fermilab E866 to higher x and provide much more precise *proton* data than is currently available.

Models based on the hypothesis that nuclear binding is governed by the exchange of mesons have been used to quite successfully describe the nuclear force. Given the success of these models, it is natural to look for direct experimental evidence for the presence of these mesons

in nuclei. Thus far, however, no direct evidence has been found. If present, these mesons will lead to an enhancement of antiquarks in the nucleus, and Drell-Yan is ideally suited to measure this enhancement. Fermilab E906 will collect data using nuclear targets, in addition to hydrogen and deuterium to look for these effects.

From deep inelastic scattering (DIS) experiments, we know that the quark level structure of a nucleon within a nucleus is different from that of a free nucleon. In the range $0.10 < x < 0.25$, a surplus of quarks (approximately 2-4%) in nuclei, known as antishadowing, is clearly observed in DIS data. To understand these phenomena, it is important to determine if it is a general property of the quark and antiquark distributions, or just a property of the valence or sea quarks. Drell-Yan, with its ability to measure sea-only quark effects, is the ideal reaction in which to measure this. Early Drell-Yan data indicate that this surplus might not be present, but with poor statistical uncertainty (3-5%). Fermilab E906's measurements will clearly determine if there is antishadowing in the sea, with statistical uncertainties of less than 1% throughout this region (see Fig. IV-16).

Using the same nuclear target data, Fermilab E906 will also study the propagation of colored partons in strongly interacting, cold nuclear matter. By comparing the Drell-Yan yields from different nuclear targets and

looking for apparent shifts in the beam parton's momentum distributions between nuclei, E906 will be able to measure the beam parton's energy loss. Previous Drell-Yan studies have placed upper limits on parton energy loss. With increased sensitivity from the 120 GeV beam and better statistical accuracy, Fermilab E906 will turn these upper limits into measurements. These measurements will aid in the understanding of jet suppression data from RHIC.

FNAL E906 is able to make these improvements over previous measurements because of the lower beam energy available at the Fermilab Main Injector. For fixed x_{beam} and x_{target} the cross section scales as the inverse of the beam energy. Thus a factor of seven more events for the same integrated luminosity can be achieved. At the same time, the primary background to the measurement, muons from J/ψ decays, decreases with increasing beam energy, allowing for an increase in instantaneous luminosity by another factor of seven. These two factors combine to provide roughly 50 times more events for the same beam time.

FNAL E906 has been approved by the Fermilab PAC and will most likely begin collecting data in late 2008. In the mean time, a number of new detector elements must be constructed, the most significant of which is a new large dipole magnet to focus the Drell-Yan muons.

D. ATOMIC TRAP TRACE ANALYSIS

d.1. ATTA for Practical ^{81}Kr and ^{85}Kr Analysis (K. Bailey, X. Du, Z.-T. Lu, P. Mueller, T. P. O'Connor, Z. El Alfy,* B. El-Kaliouby,† B. E. Lehmann,‡ R. Lorenzo,‡ R. Purtschert,‡ N. C. Sturchio,§ M. Sultan,¶ and L. Young||)

We are developing the Atom Trap Trace Analysis (ATTA) method for the analysis of two long-lived krypton isotopes, ^{81}Kr ($t_{1/2} = 2.3 \times 10^5$ years) and ^{85}Kr ($t_{1/2} = 10.8$ years). ^{81}Kr analyses can be used to determine the ages of ancient ice and groundwater in the range of 5×10^4 to 1×10^6 years; ^{85}Kr analyses can serve as a means to help verify compliance with the Nuclear Non-Proliferation Treaty.

In ATTA, atoms of the desired isotope are selectively captured into a Magneto-Optical Trap (MOT) and detected by observing the fluorescence of trapped atoms. While the principle of ATTA was demonstrated in 1999, the counting efficiency of the method realized at the time was too low for any practical applications. Since then, we have focused our effort on both

improving the efficiency and the operational reliability in order to develop a system for practical use. 1) The linear correlation between the results of ATTA and low level counting (LLC) demonstrated the validity of quantitative ATTA analyses; 2) this also provides a new measurement on the atmospheric abundance of ^{81}Kr (Fig. IV-17). Based on the slope of the correlation line and the assumption that ATTA counts ^{81}Kr and ^{85}Kr with equal efficiency, we can derive that the $^{81}\text{Kr}/\text{Kr}$ ratio is $(1.1 \pm 0.1) \times 10^{-12}$ in modern atmosphere. This value disagrees with the earlier measurements by 3-5 standard deviations. We plan to calibrate the ATTA efficiency of ^{81}Kr independent of ^{85}Kr in the near future.

With this successful demonstration, we are poised to use ATTA for its first application: to date the ancient groundwater of the Nubian Aquifer, Egypt. In 2002, a geological expedition formed by this collaboration explored the Western Desert of Egypt and extracted gas

samples at six deep groundwater sites in the region. The samples have now been reduced to nearly pure Kr by the Bern group, and will soon be analyzed using ATTA at Argonne.

*Egyptian Geological Survey and Mining Authority, Cairo, †Ain Shams University, Cairo, Egypt, ‡University of Bern, Switzerland, §University of Illinois at Chicago, ¶SUNY, Buffalo, ||Chemistry Div., ANL

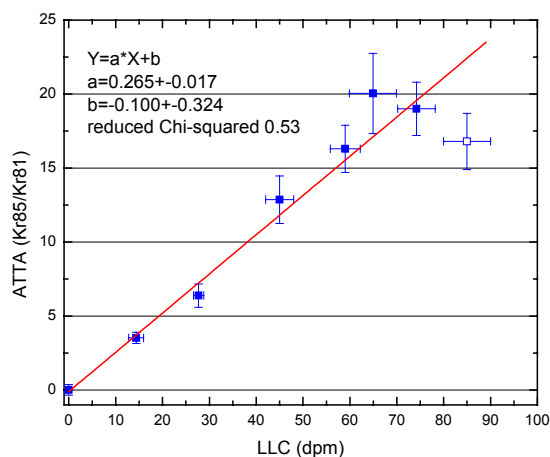


Fig. IV-17. Comparison between ATTA and LLC. In ATTA, both ^{81}Kr and ^{85}Kr atoms are counted, and the ratio of the atom counts represent the ratio of isotopic abundances. In LLC, only the decay of ^{85}Kr are counted, and the unit is decays per minute (dpm) per cm^3 of Kr at STP. The data point shown in open square represents a sample that had been severely contaminated with air in the sample preparation stage, and is not included in the fit.

d.2. ^{41}Ca Analysis for Biomedical Applications (K. Bailey, J. P. Greene, Z.-T. Lu, I. D. Moore, P. Mueller, T. P. O'Connor, L. Young,* C. Geppert,† and K. D. A. Wendt†)

We are developing an instrument for the trace analyses of ^{41}Ca based upon the Atom Trap Trace Analysis (ATTA) method. Since calcium is one of the most abundant elements in human bones and tissues, and ^{41}Ca is a long-lived isotope with very low radioactivity, ^{41}Ca as an artificial tracer is likely to find applications in bio-medicine. At present, ^{41}Ca is being studied as a tracer both in the biomedical research of bone metabolism and in the medical diagnosis of osteoporosis.

We have developed a calcium atom trap and succeeded in detecting individual ^{41}Ca atoms at the isotopic abundance level of $10^{-9} - 10^{-8}$ in biomedical samples. These samples, extracted from urine of subjects who had ingested ^{41}Ca , were provided by the Osteodiet Project, a European collaboration of physicists and medical scientists, with the aim of studying dietary strategies for osteoporosis prevention.

* Chemistry Division, ANL, †Institut für Physik, Johannes Gutenberg-Universität Mainz, Mainz, Germany

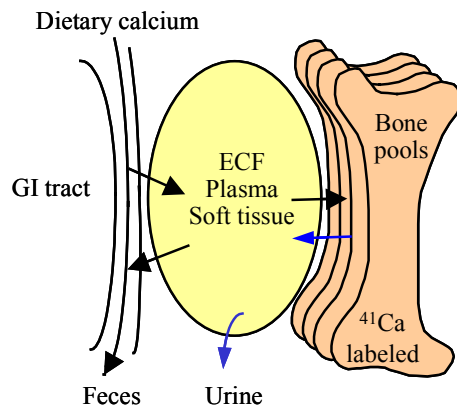


Fig. IV-18. Diagram of calcium flow in human body. ^{41}Ca is an ideal tracer for studying calcium transport in bio-systems and for measuring bone-loss rates.

d.3. Measuring the Charge Radius of ^6He (K. Bailey, J. Greene, R. J. Holt, D. Henderson, R. V. F. Janssen, C.-L. Jiang, Z.-T. Lu, I. D. Moore, P. Mueller, T. P. O'Connor, R. C. Pardo, G. T. Pennington, K. E. Rehm, J. P. Schiffer, L.-B. Wang, G. Drake,* and M. Paul†)

This collaboration aims to determine the charge radius of ^6He by measuring the atomic isotope shift of the 2^3S_1 - 3^3P_2 transition between ^4He and ^6He in the metastable 2^3S_1 level. Since ^6He atoms are short-lived and are available only in small numbers, we plan to produce the ^6He atoms at the ATLAS accelerator facility, capture individual ^6He atoms with a laser trap, and perform precision laser spectroscopy on the trapped atoms.

In the past year, we have developed a fast and efficient helium atom trap system. By measuring the fluorescence of trapped ^4He atoms, we determined that, at the ^4He injection rate of $2 \times 10^{15} \text{ s}^{-1}$, the trap can capture ^4He atoms at the rate of $2 \times 10^6 \text{ s}^{-1}$ with an efficiency of 10^{-9} . We expect that, by adding a fast gas recirculation step, the efficiency will be further improved another order of magnitude. While there are several helium trap systems already operating in

laboratories around the world, our system is unique in its design aimed for capturing short-lived helium isotopes and differ from all the existing systems in two significant ways: it takes a much shorter time ($\sim 0.1 \text{ s}$) to transfer an injected atom into the trap, and its capture efficiency is higher than conventional systems by approximately two orders of magnitude. At present, the trapping laser system at 1083 nm is complete, the spectroscopy laser system at 389 nm is under development.

Tests performed in 2001 indicate that ^6He atoms can be produced and extracted at ATLAS at the rate of $3 \times 10^6 \text{ s}^{-1}$. Combining the expected efficiency and production rate, we expect to capture ^6He in the trap at the rate of 100 per hour, which is quite sufficient for the isotope shift measurement. At present, a laser area is being prepared at the experimental area of ATLAS.

*University of Windsor, Canada, †Hebrew University, Israel.

d.4. Search for Anomalously Heavy Isotopes of Helium in the Earth's Atmosphere (R. J. Holt, Z.-T. Lu, P. Mueller, T. P. O'Connor, J. P. Schiffer, and L.-B. Wang)

Our knowledge of the stable particles that may exist in nature is defined by the limits set by measurements. There remain possibilities for 'superheavy' particles in the mass range of $10 - 10^5$ amu (atomic mass unit). There have also been suggestions that there may be very tightly bound stable states of hadronic matter. A more recent motivation for experimental searches is the possible existence of strange quark matter ('strangelets' with approximately equal numbers of up, down and strange quarks). A particularly favorable case is presented by particles of charge $+2e$, in other words helium-like particles. Normal helium is severely depleted in the terrestrial environment because of its light mass. A heavy (mass > 20 amu) and doubly-charged particle would then be helium-like but behave as other noble gases and remain in the atmosphere. The concentration of noble-gas-like atoms in the atmosphere and the subsequent very large depletion of the known light $^3,^4\text{He}$ isotopes from the atmosphere allow significantly enhanced limits to be set.

In this work, we used a laser spectroscopy technique and took advantage of the isotope shift due to the higher mass of the heavy nucleus. The signature of an anomalously heavy isotope of helium atoms would be a

resonance absorption signal occurring at a laser frequency away from the resonance of the abundant isotopes. We performed the search by probing the $1s2s\ ^3S_1 \rightarrow 1s2p\ ^3P_2$ transition at 1083 nm in helium atoms collected from the atmosphere. For the search the laser frequency was slowly scanned in the range of 20 – 109 GHz above the transition frequency of ^4He , which corresponds to a search in the mass range of 5 amu – infinity. We find at the 95% confidence level that there is no anomalous peak with an amplitude larger than 7.9×10^{-2} times the ^3He (isotopic abundance = 1.4 ppm) amplitude anywhere in the entire frequency range.

It is believed that the sun and the planets formed from the same starting material, and that this original composition is preserved in the sun. Based on the well-documented deficiency factors of noble gas elements, and assuming that the deficiency factors for the anomalous helium follow the same mass dependence, we can set limits on their abundance in the solar system (Fig. IV-19). Compared with the previous searches of such particles with mass spectrometry, this work significantly extends our knowledge over a wider range of mass and with much improved limits.

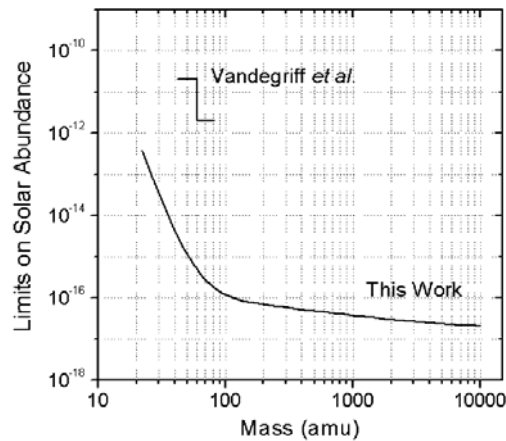


Fig. IV-19. Limits on the abundance of anomalous He-like particles in the solar system. The limits set by a previous mass-spectrometry-based search conducted by Vandegriff et al. cover the range of 42 – 82 amu. The limits set by our laser-spectroscopy-based search cover the range of 20 – 10,000 amu.

E. TESTS OF FUNDAMENTAL SYMMETRIES

e.1. Optical Trapping of Radium and the Electric Dipole Moment

(I. Ahmad, R. J. Holt, Z.-T. Lu, and E. C. Schulte)

We propose to investigate the feasibility of laser trapping and cooling of radium-225 (^{225}Ra) atoms. The realization of this proposal would enable us to measure the electric dipole moment (EDM) of ^{225}Ra and test the fundamental time-reversal symmetry (T-symmetry). The violation of time-reversal symmetry is among the most fundamental issues in physics. It is strongly believed that the underlying mechanism of the violation of T-symmetry holds the key to new physics beyond the Standard Model.

^{225}Ra is an especially good case for the search of the EDM because it has a relatively long lifetime ($t_{1/2} =$

14.9 d), has spin $1/2$ which eliminates systematic effects due to electric quadrupole coupling, is available in relatively large quantities from the decay of the long-lived ^{229}Th ($t_{1/2} = 7300$ yr), and has a well-established octupole nature. The octupole deformation increases the enhancement of the atomic EDM by increasing the Schiff moment collectively and by the parity doubling of the energy level. For example, the sensitivity to T-odd, P-odd effects in ^{225}Ra is expected to be a factor of 375 larger than in ^{199}Hg , which has been used by previous searches to set the lowest limit ($< 2 \times 10^{-28}$ e cm) so far on the atomic EDM. Work on this project is at the initial stage.

e.2. Measurement of $\sin^2\theta_W$ through Parity Violation in Deep Inelastic Scattering on Deuterium

(P. E. Reimer, J. R. Arrington, K. Hafidi, R. J. Holt, H. E. Jackson, D. H. Potterveld, E. C. Schulte, and X. Zheng)

One of the basic parameters of the Standard Model is $\sin^2\theta_W$, which represents the relative coupling strength of the weak and electromagnetic forces. The value of this parameter is predicted to vary (or run) as a function of the energy at which it is probed, Q^2 and measurement of this “running” provide strict tests of the Standard Model. At an energy equivalent to the mass of the Z-boson ($Q^2 = M_Z^2$), $\sin^2\theta_W$ is very well known, but away from this Q^2 , there are very few other measurements. Interest in measurements of $\sin^2\theta_W$ has burgeoned because of recently reported results from the NuTeV collaboration at Fermilab, which found a *three standard deviation* difference with the Standard Model in their neutrino-iron measurement of $\sin^2\theta_W$ at $Q^2 \approx 20$ GeV 2 . The asymmetry from parity violation in electron-deuterium deep inelastic scattering (DIS) is proportional to $\sin^2\theta_W$, and relatively large ($A_d \approx 10^{-4} Q^2$), making it quite accessible experimentally. Historically, DIS parity violation from a deuterium target was first observed by Prescott *et al.* in the mid-1970's and was used to establish the Weinberg-Salam model. Investigations are underway to repeat this experiment, focusing on facilities at an upgraded 12 GeV Jefferson Laboratory (and possibly at SLAC). In a relatively short experiment, a DIS parity violation experiment could achieve the statistical sensitivity needed to investigate the NuTeV result, and using a deuterium target, it should not suffer from the uncertainties in nuclear effects and nuclear parton distributions unlike the NuTeV iron measurement.